VOLTAGE STABILITY IMPROVEMENT USING ARTIFICIAL NEURAL NETWORK CONTROLLED UNIFIED POWER FLOW CONTROLLER (UPFC)

ARIEL MUTEGI MBAE

MASTER OF SCIENCE

(Electrical Engineering)

JOMO KENYATTA UNIVERSITY OF AGRICULTURE AND TECHNOLOGY

2017

Voltage Stability Improvement Using Artificial Neural Network Controlled Unified Power Flow Controller (UPFC)

Ariel Mutegi Mbae

A thesis submitted in partial fulfillment for the degree of Master of Science in Electrical Engineering in the Jomo Kenyatta University of Agriculture and Technology

2017

DECLARATION

This thesis is my original work and has not been presented for a degree in any other University

Signature…… Date……. ……..

Ariel Mutegi Mbae

This thesis has been submitted for examination with our approval as University Supervisors

Signature…… Date……. ……..

Dr. P.K Kihato, PhD

JKUAT, Kenya

Signature…… Date……. ……..

Dr. C.M Muriithi, PhD

TUK, Kenya

Signature…… Date……. ……..

Dr. M.J Saulo, PhD

TUM, Kenya

DEDICATION

To my wife and kids

ACKNOWLEDGEMENT

I wish to acknowledge the efforts of my supervisors in guiding and encouraging me through this research. I have to accept it was tough and without them I would have given up. My family has stood by me through thick and thin. Thank you all for your support.

TABLE OF CONTENTS

LIST OF TABLES

LIST OF FIGURES

APPENDICES

LIST OF ABBREVIATIONS

ANN	Artificial Neural Networks
ANFIS	Adaptive Neuro-Fuzzy Inference System
DC	Direct Current
DFC	Dynamic Flow Controller
FACTS	Flexible Alternating Current Transmission Systems
FVSI	Fast voltage Stability Index
GWh	Giga Watt Hours
HVDC	High-Voltage Direct Current
B2B	Back-to-Back
IEEE	Institute of Electrical and Electronics Engineers
IGBT	Insulated Gate Bipolar Transistor
IPFC	Interline Power Flow Controller
kV	Kilovolts
LSI	Line Stability Index

MVA	Mega Volt Ampere
MW	Mega Watts
P-V	Active Power-Voltage
Q-V	Reactive Power-Voltage
STATCOM	Static Synchronous Compensator
SSSC	Static Synchronous Series Compensator
SVC	Static Var Compensator
TCSC	Thyristor Controlled Series Compesator
UPFC	Unified Power Flow Controller
VSC	Voltage Source Converters

ABSTRACT

The demand for clean, reliable and affordable energy is growing at unprecedented rates across the world. As we seek to increase the quantity of energy produced, the supply quality challenges will grow in tandem. The growing long distances between generation and load centers only serve to compound the voltage stability challenge. Due to their versatility, high speed control and flexibility, FACTS (Flexible Alternating Current Transmission System) devices have been increasingly used as an alternative to the conventional methods such as capacitor banks and reactors over the years. However, for maximum benefits to be reaped from the said devices, their optimal location within a power network is a critical consideration. Research on the location of the FACTS devices using such methods as small signal analysis, hopf bifurcation, time domain analysis, loss sensitivity factors, fuzzy index, voltage change index as well as voltage stability index has been well documented. This has been coupled with various FACTS devices control strategies such as genetic algorithm, particle swarm optimization, pulse width modulation and runge-Kutta method. Over and above the optimal location of the UPFC, this research sought to use artificial neural networks as a way of replacing human system control operators so as to improve on real time system control as opposed to time delays experienced in relaying and actioning of instructions. A Voltage Security Constrained load flow analysis was done on the 10-Generator 39-Bus IEEE test system. This was followed by optimal placement of the UPFC using voltage stability indices after which an analysis of the voltage stability improvement was done. After that, an artificial neural network was trained to help track voltage profiles at various buses and issue instructions to the UPFC so as to stabilize voltages. Finally, a cost-benefit analysis of the proposed system showed that indeed the developed system is an economically viable option in the improvement of voltage profiles in a power system. A 100MVA UPFC led to an overall voltage stability improvement in the network. This was quantified by an overall loss reduction by 1.217MW.The developed control system was able to track voltage profiles at various buses and issue instructions to the UPFC to either absorb or inject reactive power so as to improve on the voltage profile.

CHAPTER ONE

INTRODUCTION

1.1 Overview

Recent blackouts around the world are mainly due to voltage collapse in stressed power systems associated with low voltage profiles, heavy reactive power inflows, inadequate reactive power support and heavy loading. Voltage collapse requires time for system restoration with customers going for a long time with no power supply. Therefore, the study of voltage stability is one of the major concerns in power system operation and planning. This presents power system engineering practitioners with the challenge of coming up with ways and means of maintaining the required system voltage profiles. Proper knowledge of how close the actual system's operating voltages are from the voltage stability limits is crucial to system operators. Therefore voltage stability indices are crucial parameters for many voltage stability studies as they provide critical information about the proximity to voltage instability in a power system (Kundur, 1994; Co. P. S., 2012).

Conventional voltage stability improvement ways such as capacitor banks, reactors and transformers can be used to provide steady state voltage control. However, these devices are based on electro-mechanical control among other drawbacks thus impeding high speed control. This in essence means that they lack the much sought after traits of operational flexibility and versatility. FACTS devices regulate the active and reactive power as well as adapting to voltage magnitude control simultaneously because of their

flexibility and fast control. Placement of these devices in optimal locations leads to control of power flow and maintenance of bus voltages in desired level and thus improving voltage stability margins as well as keeping system operational costs at a minimum.

Human operators are slow to act on voltage profiles information in real time thus impede the maximum usage of the operational versatility of the FACTS devices. For this reason, it is necessary to continuously couple the FACTS devices with artificial intelligence techniques that can act in real time.

The main difference between artificial neural networks and a conventional computer system is the massive parallelism, distributed representation, redundancy and a good fault tolerance which they exploit in order to deal with the unreliability of the individual computing units. They have the ability to synthesize complex mappings accurately and rapidly as is the case with a real power system due to the complex interdependence of various operating parameters.

1.2 Problem Statement

Conventional voltage stability improvement methods such as capacitor banks, reactors and transformers can be used to provide steady state voltage control. However, these devices are based on electro-mechanical control among other drawbacks explained later thus impeding high speed voltage control.

FACTS devices provide a better adaptation to varying operational conditions and improvement on the usage of existing installations in power systems by using power electronic controllers. Their main advantages over the conventional methods are that the devices are both dynamic-fast controllability using power electronics- and static-no moving parts to perform the dynamic controllability. Optimal placement of FACTS devices so as to take care of the twin objectives of voltage security and system economy was a key issue after the load flow solution.

This research sought to come up with a new way of voltage stability improvement using FACTS devices by solving the challenge of reactive power absorption and generation using artificial neural network trained control system for real-time control.

1.3 Justification

Power systems are increasingly becoming more overloaded and constantly being operated close to their voltage stability limits. Voltage stability is the ability of a power system to maintain acceptable voltage levels under normal operating conditions and after being subjected to disturbances such as a sudden increase in load or loss of a major generation plant. Major national power outages have been documented in the recent past in countries such as Kenya, USA, France, Belgium, Sweden and Japan.

The rise in the use of FACTS devices for voltage stability improvement has been a growing trend due to the huge capital outlay required to construct new transmission and distribution lines, pressure on land as well as environmental concerns worldwide. This has also been fuelled by the inherent drawbacks of the convectional techniques e.g.

capacitor banks, namely lack of versatility and flexibility, being electromechanical thus slow to act among others.

Coupling the FACTS devices with artificial intelligence methods will go a long way in voltage stability improvement. This research uses artificial neural networks which mimic biological nervous systems as a way of trying to replace human operators who are at times slow to relay and act on information on system voltage profiles thus leading cascaded system voltage collapse.

1.4 Objectives

1.4.1 General Objective

The main objective of this research is to analyze the static voltage stability improvement of a power system using artificial neural networks controlled Unified Power Flow Controller (UPFC).

1.4.2 Specific Objectives

(i) To perform a security constrained load flow solution on the IEEE 39-bus test system.

(ii) To do an optimal placement of UPFC in the IEEE 39-bus test system.

(iii) To develop artificial neural networks trained control system for the UPFC in voltage stability improvement.

(iv) To perform a cost-benefit analysis of the developed voltage control system.

1.5 Scope

The scope of this research was limited to the IEEE 39-Bus,10-Generator test system. A voltage security-constrained load flow analysis was carried out in the PSAT test system that ran on MATLAB'S Simulink environment. The optimal location of FACTS devices was carried out using two static voltage stability indices namely the Fast Voltage Stability index and the Line stability index.

A reactive power injection and absorption control strategy that uses Artificial Neural Networks was developed in Simulink and finally a project viability appraisal for the proposed system was carried out.

1.6 Thesis Organization

Chapter 1

This chapter presents an introduction of the research work, outlines the problem statement, gives a justification for the research work and finally the goals of the work.

Chapter 2

This chapter presents a literature review on the conventional methods of voltage-reactive power control, why FACTS devices are increasingly being used for reactive power control, a discussion on UPFC in particular, a review of recent works related to the use of UPFC in reactive power control, ANN and finally a discussion on investment appraisal methodology.

Chapter 3

This chapter gives the methodology followed in carrying out this research work.

Chapter 4

This chapter presents the results obtained and an analysis and discussion of the same against the objectives of the research.

Chapter 5

This chapter presents a conclusion of the work and gives recommendations and/or gaps for future research.

1.7 Conference and Journal Papers Published from this Research

From this research, the following two conference papers and one journal paper have been published;

1. Mutegi, AM, Maina, CM and Saulo, MJ,"A Review on Voltage Stability Improvement using Artificial Neural Networks Controlled FACTS devices", in *Sustainable Research and Innovation Conference (SRI)*,Nairobi,2015, pp. 288-293.
2. Mutegi, AM,, Kihato, PK, Maina, CM and Saulo, MJ," Optimal Placement of FACTS devices using Voltage Stability Indices", in *Sustainable Research and Innovation Conference (SRI)*,Nairobi,2016, pp. 138-143.
3. Mutegi, AM ,Kihato, PK, Maina, CM and Saulo, MJ,"Voltage Stability Indices Improvement on Optimal Placement of FACTS devices,"Eur.*Journal of Adv. in Eng. and Tech.,*vol.03,issue.07, pp.9-15,Aug.2016.

CHAPTER TWO

LITERATURE REVIEW

2.1 Reactive Power and Voltage Control

2.1.1 Overview

Reactive power is needed in order to maintain the voltage to deliver active power through power lines. It results from energy storage in the grid due to system inductance and capacitance. Motor loads and other loads require reactive power to convert the flow of electrons into useful work. When there is not enough reactive power, the voltage sags down and it is not possible to push the power demanded by loads through the lines (Kundur, 1994; Co. P. S., 2012) (National Laboratory of Engineering Science and Technology, 2011).

Transformers and transmission lines introduce inductance as well as resistance. We must raise the voltage higher to push the power through the inductance of the line.The further the transmission of power, the higher the voltage needs to be raised because of increased line impedance.

The flow of reactive power from the supplies to the loads causes additional heating of the lines and voltage drops in the network. One dilemma with reactive power is that a sufficient quantity of it is needed to provide the loads and losses in the network. However having too much reactive power flowing around the network causes excess

heating and undesirable voltage drops. To solve this, reactive power sources are placed exactly at the location where the reactive power is needed (USAID, 2010).

The objective of voltage and reactive power control is to ensure that voltages at the terminals of all equipment in the system are within the acceptable operating limits and to minimize reactive power flow so as to reduce the heating losses.

2.1.2 Production and Absorption of Reactive Power

There are several methods used in the production and absorption of reactive power all geared towards regulation of supply voltage levels to the required limits.

Synchronous generators can generate (when over-excited) or absorb (when under-excited) reactive power depending on the capability curve of each machine (Kundur, 1994).

Overhead lines and underground cables are able to supply or absorb reactive power depending on the load current whereby below surge impedance load, they supply and above surge impedance load, they absorb reactive power (Kundur, 1994).

Transformers always absorb reactive power regardless of their loading; at no load, the shunt magnetizing reactance effects dominate and at full load, the series leakage inductance effects dominate (Kundur, 1994).

A typical consumer load bus supplied by a power system is composed of a large number of devices. The composition changes depending on the day, season and weather

conditions. The composite characteristics are normally such that a load bus absorbs reactive power. Both active and reactive powers of the composite loads vary due to voltage magnitude (Kundur, 1994).

Shunt capacitors supply reactive power thus boosting local voltages. The principal advantages of shunt capacitors are their low cost and flexibility of installation and operation. The main disadvantage of shunt capacitors is that their reactive power output is proportional to the inverse of the square of the voltage. Thus their usefulness decreases when they are most needed (Kundur, 1994) (University C. , 2009).

Static series capacitors are connected in series with line conductors to reduce the inductive reactance between supply and load for improved power transfer capability. The drawbacks of series capacitors are ferro resonance switching in of unloaded transformer at the end of a series compensated line and locking of induction motors (Kundur, 1994) (University C. , 2009).

A synchronous condenser is a synchronous motor running without a prime mover or a mechanical load which by controlling the field excitation can be made to either generate or absorb reactive power. For proper voltage control, the synchronous motor is used hand in hand with a voltage regulator. The condenser is flexible to operate for all load conditions and its reactive power output is not a function of system voltage. However, synchronous condensers are expensive to install and it is difficult to increase their capacity.

2.1.3 Facts Devices

FACTS devices is an acronym used to describe a wide range of controllers, many of them incorporating large power electronic converters, which may be used to increase the flexibility of power systems and thus make them more controllable. They are defined as alternating current transmission systems incorporating electronic-based and other static controllers to enhance controllability and increase power transfer capability. FACTS devices can regulate the active and reactive power control as well as adapting to voltage magnitude control simultaneously because of their increased versatility and fast real time control.

In shunt compensation, the power system is connected in shunt with the FACTS device and works as a controllable current source.

The general power transfer equation is:

$$P = \frac{EV}{X}\sin(\delta) \qquad (2.1)$$

Whereby P=Delivered active power,E=Sending end voltage,V=Terminal voltage, δ =power angle and X = line reactance.

In the case of a lossless line-perfectly matched line, voltage magnitude at the receiving end is the same as voltage magnitude at the sending end i.e.

$$V_s = V_r = V \qquad (2.2)$$

Transmission line reactance results in a phase lag δ that depends on line reactance X thus:

$$V_s = V\cos(\frac{\delta}{2}) + jV\sin(\frac{\delta}{2}) \tag{2.3}$$

$$V_r = V\cos(\frac{\delta}{2}) - jV\sin(\frac{\delta}{2}) \tag{2.4}$$

$$I = \frac{V_s - V_r}{jX} = \frac{2V\sin(\frac{\delta}{2})}{X} \tag{2.5}$$

As it is a no-loss line, active power P is the same at any point of the line:

$$P_s = P_r = P = V\cos(\frac{\delta}{2}).\frac{2V\sin(\frac{\delta}{2})}{X} = \frac{V^2}{X}\sin(\delta) \tag{2.6}$$

Reactive power at sending end is the opposite of reactive power at receiving end:

$$Q_s = -Q_r = Q = V\sin(\frac{\delta}{2}).\frac{2V\sin(\frac{\delta}{2})}{X} = \frac{V^2}{X}(1-\cos\delta) \tag{2.7}$$

As δ is very small, active power mainly depends on δ whereas reactive power mainly depends on voltage magnitude.

FACTS devices for series compensation modify line impedance whereby X is decreased by X_C so as to increase the transmittable active power. However, more reactive power

must be provided;

$$P = \frac{V^2}{X - X_C}\sin(\delta) \tag{2.8}$$

$$Q = \frac{V^2}{X - X_C}(1 - \cos\delta) \tag{2.9}$$

In shunt compensation, reactive current is injected into the line to maintain voltage magnitude. Transmittable active power is increased but more reactive power is to be provided.

$$P = \frac{2V^2}{X}\sin(\frac{\delta}{2}) \tag{2.10}$$

$$Q = \frac{2V^2}{X}\left[1 - \cos(\frac{\delta}{2})\right] \tag{2.11}$$

Examples of FACTS devices are Voltage-Sourced Converters, Static Shunt Compesators, Static Compesators, Thyristor-Controlled Series Capacitor, Static Synchronous Series Compesator, Interline Power Flow Controller and High Voltage direct current devices (Gyugyi, 2000).

TCSC are used to address dynamic problems in transmission lines by increasing damping when large electrical systems are interconnected. Their high speed switching capability provides a mechanism for controlling line power flow which permits increased loading of existing transmission lines and allows for rapid readjustment of line

power flow in response to various contingencies. It can also regulate the steady-state power flow within its rating limits.

The DFC is a hybrid between a phase shift transformer and a mechanically switched shunt capacitor. The capacitor provides voltage support in case of overload in a manner to result in a desired stepped reactance variation. The phase shift transformer injects a voltage in quadrature with the node voltage.

The IPFC is used to control the power flow of two lines starting in one substation to optimize the network utilization. It consists of two series VSCs whose DC capacitors area coupled. This allows the active power to circulate between the VSCs.Due to its complex setup, specific application cases need to be identified in order to justify the investment.

Back to back devices provide full power flow controllability and power flow limitation thus overload of these devices is not possible. They resist cascaded outages which occur due to thermal overloads of the lines.

HVDC B2B is mainly used when two asynchronous networks need to be coupled. The HVDC VSC B2B on the other hand provides full voltage controllability on networks.

The SVC and STATCOM are static var generators whose output is varied so as to control specific parameters of the power network. Static compensation is mainly used to increase power transmission capability in a given power network by voltage control. i.e. The reactive power output of the compesator is varied to control the voltage at given terminals of the network so as to maintain the desired power flow.

The SSSC is used for shunt and series compensation as well as for transmission angle control by acting as a series voltage source. It does this by injecting capacitive or inductive compensating voltage in series with the line irrespective of the line current up to its specified current rating.

The UPFC is a combination of a static compensator (STATCOM) and static series compensator (SSSC).It acts as a shunt compensating and a phase shifting device simultaneously thus making it one of the most versatile and complex FACTS devices. It provides simultaneous and real-time control of all basic power system parameters-reactive power, transmission voltage, impedance and phase angle. The UPFC uses solid state devices which provide functional flexibility generally not attainable by conventional thyristor controlled systems (Gyugyi, 2000; Kulkarni, 1998).

The UPFC consists of two voltage source converters as illustrated below (University C. , 2009; Gyugyi, 2000; Kulkarni, 1998; Kumar, 2011; Renz, 1999).

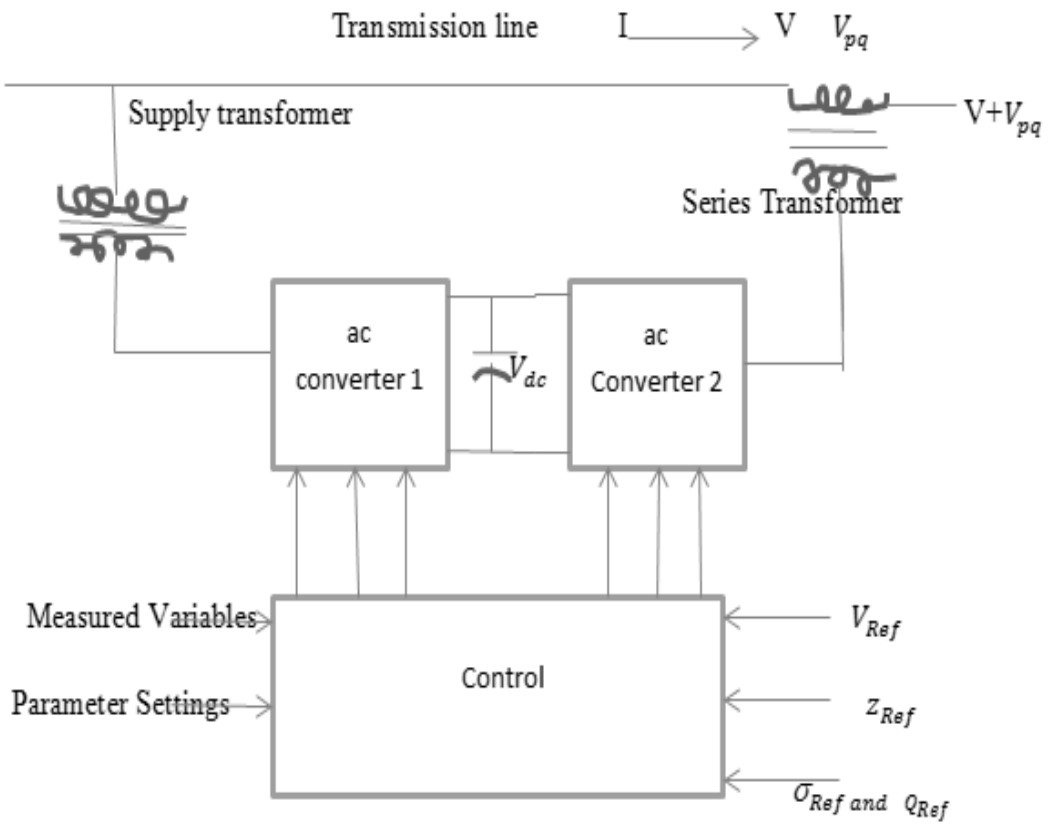

Figure 2.1: Schematic of a UPFC

The shunt inverter (STATCOM) is used for voltage regulation at the point of connection by injecting an opportune reactive power flow into the line and to balance the real power flow exchanged between the series inverter (SSSC) and the transmission line. The series inverter can be used to control the real and reactive line power flow by inserting an opportune voltage with controllable magnitude and phase in series with the transmission line.

These back-to-back converters are operated from a common dc link provided by a dc storage capacitor. This works as an ideal ac-to-ac power converter in which the real

power freely flows in either direction between the ac terminals of the two converters and each converter can independently generate or absorb reactive power on its own ac output terminal.

Converter 2 provides the main function of the UPFC by injecting a voltage V_{pq} with controllable magnitude V_{pq} and a phase angle ρ in series with the line through an insertion transformer. This injected voltage acts as a synchronous ac voltage source. Converter 1 supplies or absorbs the real power demanded by converter 2 at the common dc link to support the real power exchange resulting from the series voltage injection. This dc link power demand of converter 2 is converted back to ac by converter 1 and coupled to the transmission line bus via a shunt connected transformer. Converter 1 can also generate or absorb controllable reactive power and thereby provide independent shunt reactive compensation for the line.

The UPFC power flow control capability can be illustrated by the real and reactive power transmission versus transmission angle characteristics of the simple two-machine system shown below.

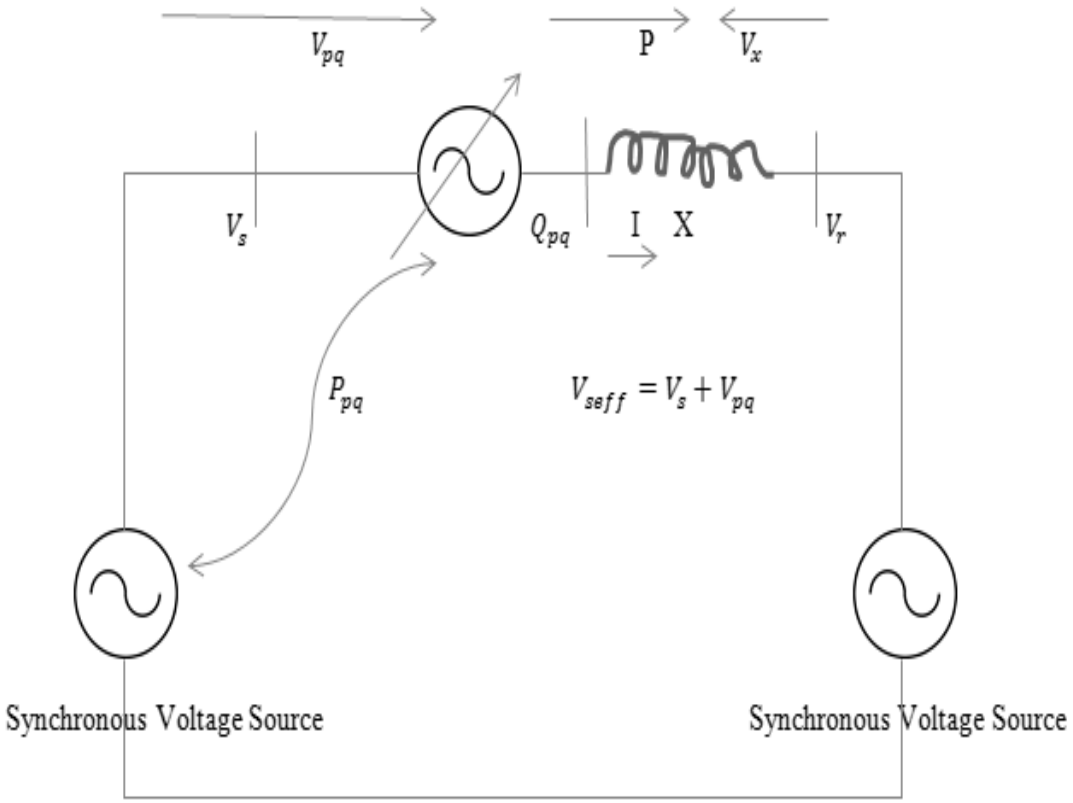

Figure 2.2: Two-Machine UPFC Model

The UPFC is a generalized synchronous voltage source (SVS) represented at the fundamental frequency by voltage phasor V_{pq} with a controllable magnitude $0 \leq V_{pq} \leq V_{pqmax}$ and phase angle $0 \leq \rho \leq 2\pi$ in series with the transmission line.The transmitted power P and the reactive power $-jQ_r$ supplied to the receiving end can be expressed as:

$$P - jQ_r = V_r\left(\frac{V_s + V_{pq} - V_r}{jX}\right)^* \qquad (2.12)$$

If $V_{pq} = 0$, then (2.12) describes the uncompensated system.

$$P - jQ_r = V_r(\frac{V_s - V_r}{jX})^* \tag{2.13}$$

Thus with $V_{pq} \neq 0$, the total real and reactive power can be written as:

$$P - jQ_r = V_r(\frac{V_s - V_r}{jX})^* + \frac{VrV_{pq}^*}{-jX} \tag{2.14}$$

Substituting

$$V_s = Ve^{j\delta/2} = V(\cos\frac{\delta}{2} + j\sin\frac{\delta}{2}) \tag{2.15}$$

$$V_r = Ve^{-j\delta/2} = V(\cos\frac{\delta}{2} - j\sin\frac{\delta}{2}) \tag{2.16}$$

and

$$V_{pq} = V_{pq}e^{j(\frac{\delta}{2}+\rho)} = V_{pq}\{\cos(\frac{\delta}{2}+\rho) + j\sin(\frac{\delta}{2}+\rho)\} \tag{2.17}$$

the following expressions are obtained for P and Q:

$$P(\delta,\rho) = P_o(\delta) + P_{pq}(\rho) = \frac{V^2}{X}\sin\delta - \frac{VV_{pq}}{X}\cos(\frac{\delta}{2}+\rho) \tag{2.18}$$

and

$$Q_r(\delta,\rho) = Q_{or}(\delta) + Q_{pq}(\rho) = \frac{V^2}{X}(1-\cos\delta) - \frac{VV_{pq}}{X}\sin(\frac{\delta}{2}+\rho) \tag{2.19}$$

where $P_o(\delta) = \frac{V^2}{X}\sin\delta$ and $Q_{or}(\delta) = -\frac{V^2}{X}(1-\cos\delta)$ are the real and reactive power characterizing the power transmission of the uncompensated system at a given angle δ.Since angle ρ is freely variable between 0 and 2π at any given transmission angle $\delta(0 \leq \delta \leq \pi)$,it follows that $P_{pq}(\rho)$ and $Q_{pq}(\rho)$ are controllable between $-\frac{VV_{pq}}{X}$ and

$+\frac{VV_{pq}}{X}$ independent of angle δ.This is done by the series inverter 2 that injects a voltage with controllable magnitude and a phase angle ρ in series with the line through an insertion transformer.

Therefore, the transmittable real power P is controllable between $-\frac{VV_{pq\max}}{X}$ and $+\frac{VV_{pq\max}}{X}$ i.e.

$$P_o(\delta)-\frac{VV_{pq\max}}{X}\le P_o(\delta)+\frac{VV_{pq\max}}{X} \qquad (2.20)$$

and the reactive power Q_r is controllable between:

$$Q_{or}(\delta)-\frac{VV_{pq\max}}{X}\le Q_{or}(\delta)\le Q_{or}(\delta)+\frac{VV_{pq\max}}{X} \qquad (2.21)$$

at any transmission angle δ .

The wide range of control for the transmitted power that is independent of the transmission angle δ indicates the superior capability of the UPFC in power flow control. The UPFC control is based on the vector-control approach, whereby, vector represents a set of three instantaneous phase variables that sum to zero (Renz, 1999; Nizam, 2006).

For the purposes of power control it is useful to view these vectors in an orthogonal co-ordinate system with p and q axes such that the p-axis is always coincident with the instantaneous voltage vector v and the q-axis is in quadrature with it.

The UPFC control system is divided into internal/converter control and functional operation control. The internal controls operate the two converters so as to produce the

commanded series injected voltage and simultaneously draw the desired shunt reactive current. The series converter responds directly and independently to the demand for series voltage vector injection. Thus changes in the series voltage vector v_{pq} can therefore be affected virtually instantaneously.

On the other hand, the shunt converter operates under a closed-loop current control structure whereby the shunt real and reactive power components are independently controlled. The shunt reactive power responds directly to an input demand. However, the shunt real power is dictated by another control loop that acts to maintain a preset voltage level on the dc link, thereby providing the real power supply/sink needed for the support of the series voltage injection. The converters do not exchange reactive power through the link.

The external operation control defines the functional operating mode of the UPFC and is responsible for generating the internal references, v_{pqRef} and i_{qRef}, for the series and shunt compensation to meet the prevailing demands of the transmission system. The functional operating modes and compensation demands can be set manually by the operator or dictated by an automatic system optimization control to meet specific operating and contingency requirements.

2.2 Voltage Stability Indices

Voltage stability is the ability of a power system to maintain acceptable voltage levels at all buses in the system under normal operating conditions and after being subjected to a disturbance (Kundur, 1994).

The study of voltage stability is done under different approaches that can be basically classified into dynamic and static analysis. Dynamic analysis is done using models characterized by nonlinear differential and algebraic equations which include generator dynamics, induction motors and tap changing transformers. They apply real-time simulation in time domain using precise dynamic models.

Static methods solve specific first or second order functions or indices derived from basic power flow equations of the network which show the capability of the power system to remain stable. They run with specific load increases until the voltage collapse point is reached thus allowing the examination of a wide range of system operating conditions such as heavy loading and contingencies.

We can broadly classify voltage stability indices (VSI) into two, namely the Jacobian matrix VSI and the system variables based VSI. Jacobian matrix based VSI can calculate the voltage collapse point and determine the voltage stability margin but their computation time is high hence not good for online assessment. On the other hand, system variables based VSI, which use the elements of the admittance matrix and some system variables such as bus voltages or power flow through lines, require less computation and are thus adequate for online monitoring and fast diagnosis of system conditions and contingency ranking thus used in this research work.

There are many system variable based VSI such as the L index, voltage collapse index, voltage index, line stability indices and voltage collapse point indicators. In this research, we used two reactive power adjustment static methods namely the Fast Voltage

Stability (FVSI) and the Line Stability indices (LSI) because the research work centred on reactive power-voltage balance in a power system.

The Fast Voltage Stability Index – FVSI-is an indicator based on measurements of voltages and reactive power. It is a very good indicator of the weakest lines in the network for mitigation such as placement of FACTS devices. The two-bus line model used to derive the indicator is shown below:

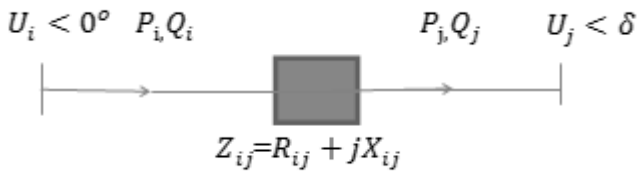

Figure 2.3: Two-Bus Line Model

We have two Buses namely Bus i (sending) and Bus j (receiving). U_i is the sending end voltage, Q_j the reactive power at the receiving end. Bus i is used as the reference bus, with the voltage angle set to zero. The derivation of the index begins with the general equation for the current in a line between two

buses i and j as:

$$I_{ij} = \frac{u_i - u_j}{z_{ij}} \qquad (2.22)$$

The apparent power received at bus j is found by multiplying (2.22) with the voltage at bus j as:

$$I_{ij} = u_j(\frac{u_i - u_j}{z_{ij}})^* = P_j + jQ_j \tag{2.23}$$

The imaginary part of (2.23) is the reactive power received at bus j given by equation:

$$Q_j = \frac{u_i u_j(R_{ij}\sin\delta + X_{ij}\cos\delta) - X_{ij}u_j^2}{R_{ij}^2 + X_{ij}^2} \tag{2.24}$$

This can be rewritten as a second-order equation for u_j as:

$$u_j^2 - u_j u_i(\frac{R_{ij}}{X_{ij}}\sin\delta + \cos\delta + (X_{ij} + \frac{R_{ij}^2}{X_{ij}})Q_j \tag{2.25}$$

FVSI is based on the principle that the system remains stable as long as there are only real solutions to equation (2.25) above.

i.e.

$$\left[(\frac{R_{ij}}{X_{ij}}\sin\delta + \cos\delta)u_i\right]^2 - 4(X_{ij} + \frac{R_{ij}^2}{X_{ij}})Q_j \geq 0 \tag{2.26}$$

Simplifying (2.26) above and assuming that the angle difference δ is normally very small (δ≈0, $R_{ij}\sin\delta\approx 0$ and $X_{ij}\cos\delta\approx X_{ij}$) gives:

$$(X_{ij}u_i)^2 \geq 4X_{ij} + R_{ij}^2)Q_j \qquad (2.27)$$

FVSI is thus defined as the ratio between the two terms above giving;

$$FVSI = \frac{4Z_{ij}^2 Q_j}{u_i^j X_{ij}} \leq 1 \qquad (2.28)$$

As shown in equation (2.28), the power transmission through line i-j is stable as long as

$$FVSI_{ij} \leq 1$$

LSI resembles FVSI based on the power flow equation for a transmission line.From equation (2.24) above and replacing $R + jX$ by Z<θ, gives an expression for the received reactive power at bus j:

$$Q_j = \frac{u_i u_j}{Z_{ij}}\sin(\theta-\delta) - \frac{u_j^2}{Z_{ij}}\sin\theta \qquad (2.29)$$

Picking from (2.23), the receiving-end voltage can be expressed as a second-order equation:

$$u_j^2 \sin\theta - u_j u_i \sin(\theta - \delta) - Q_j Z_{ij} = 0 \qquad (2.30)$$

Just as with FVSI,the system remains stable as long as there are only real solutions to equation (2.30) above.

Rearranging the equation and using the fact that $Z_{ij}\sin\theta = X_{ij}$ gives the equation for the line stability as:

$$LSI = \frac{4X_{ij}Q_j}{u_i^2 \sin^2(\theta - \delta)} \leq 1 \qquad (2.31)$$

The similarity of the two indicators can be illustrated by inserting $\delta = 0$ in equation (2.31) above to give:

$$LSI = \frac{4X_{ij}Q_j}{u_i^2 \sin^2(\theta)} = \frac{4Z_{ij}Q_j}{u_i^2 X_{ij}} = FVSI \quad \text{for} \quad \delta = 0 \qquad (2.32)$$

Thus the only difference between LSI and FVSI is that LSI accounts for the voltage angle difference which FVSI assumes to be zero. This is also the advantage of FVSI over LSI as it only requires measurements of magnitudes only whereas LSI requires synchronized phasor measurements at both line ends.

2.3 Artificial Intelligence

Artificial intelligence refers to the development of systems equipped with the ability and characteristics of a human being. This includes the ability to think, reason out, find meaning, generalize, distinguish, learn from the past experience and to rectify their mistakes.

Artificial intelligence has been necessitated by the fact that power system analysis by convectional techniques is becoming increasingly difficult because of the complexity, versatility and large amounts of information that needs to be computed, diagnosed and learnt over a short period of time.

Some of the common artificial intelligence techniques include but not limited to fuzzy logic, expert systems, neural networks, genetic algorithm and hybrids of any of the above.

Fuzzy systems have an ability to produce exact and accurate solutions from certain or even approximate data. They have superior expressive power, higher generality and an improved capability to model complex but fairly linear problems.

Expert systems obtain the knowledge of a human expert in a narrow specified domain into a machine implementable form. The knowledge is stored as rules, decision trees, models and frames. They are unable to learn or adapt to new situations thus not suitable for many power system applications.

Genetic algorithm is an optimization technique based on the study of natural selection and natural genetics whereby the fittest individual in a population has the highest probability and possibility for survival.

Artificial Neural networks are used to improve the performance of the line. They are trained to change the values of line parameters such as voltages over a given range just as a human being will do thus their choice for this research work.

2.3.1 Artificial Neural Networks

An Artificial Neural Network (ANN) is an information processing paradigm that is inspired by the way biological nervous systems process information.

In the human brain, a typical neuron collects signals from others through a host of fine structures called dendrites. The neuron sends out spikes of electrical activity through a long, thin strand known as an axon, which splits into thousands of branches. At the end of each branch, a structure called a synapse converts the activity from the axon into electrical effects that inhibit or excite activity from the axon into electrical effects that inhibit or excite activity in the connected neurons. When a neuron receives excitatory input that is sufficiently large compared with its inhibitory input, it sends a spike of electrical activity down its axon. Learning occurs by changing the effectiveness of the synapses so that the influence of one neuron on another changes (G.Tulasiram, Simulation of real and reactive power flow control with UPFC connected to a transmission line, 2008) (University L. , 2009) (University L. , 2001) (Siganos, 2009)

The figure below shows the structure of an abstract neuron with n inputs. Each input channel i can transmit a real value x_i :

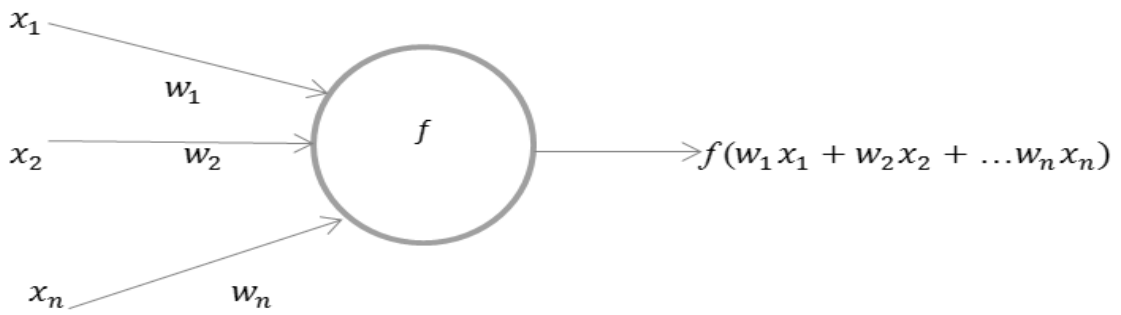

Figure 2.4: An abstract Neuron with *n* inputs

The primitive function *f* computed in the body of the abstract neuron can be selected arbitrarily. The input channels have an associated weight, which means that the incoming information x_i is multiplied by the corresponding weight w_i.The transmitted information is integrated at the neuron and the primitive function is then evaluated.

The perceptron is the simplest form of a neural network used for the classification of a special type of patterns that are linearly separable. It consists of a single McCulloch-Pitts neuron with adjustable synaptic weights and bias.

If the patterns used to train the perceptron are drawn from linearly separable classes, then the perceptron algorithm converges and positions the decision surface in the form of a hyper plane between the classes.

The single-layer perceptron shown below has a single neuron:

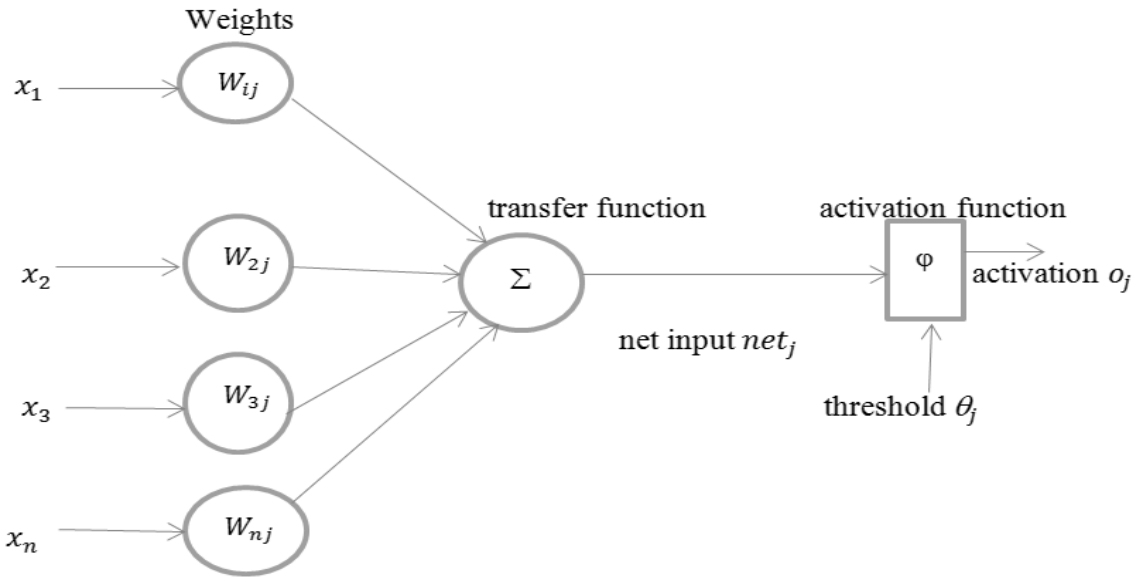

Figure 2.5: Single Layer Perceptron

A signal x_n at the input of synapse *n* connected to neuron *j* is multiplied by the synaptic weight w_{nj}.The weight w_{nj} is positive if the associated synapse is excitatory and negative if the synapse is inhibitory.

Normally, we try to use very simple primitive functions of one argument at the nodes. This means that the incoming *n* arguments have to be reduced to a single numerical value. Therefore, computing units are split into two functional parts; an integration function ∑ reduces the *n* arguments to a single value and the output or activation function φ produces the output of this node taking that single value as its argument. Normally ∑ is an addition function.

A neuron *k* is modelled by the following pair of equations:

$$v_k = \sum_{j=0}^{p} w_{kj} x_j \tag{2.33}$$

$$y_k = \varphi(v_k) \tag{2.34}$$

or in matrix form

$$v_k = [w_{ko} w_{k1} \ldots\ldots\ldots w_{kp}] \begin{pmatrix} x_0 \\ x_1 \\ \vdots \\ x_p \end{pmatrix} = w_k^T x \tag{2.35}$$

There are various types of activation functions examples of which are threshold activation function, piecewise-linear activation function, sigmoid activation function, hyperbolic tangent function and softmax activation function.

Among the many interesting properties of a neural network is the ability of the network to learn from its environment and to improve its performance through learning. A neural network learns about its environment through an iterative process of adjustments applied to its synaptic weights and thresholds.

A learning algorithm is an adaptive method by which a network of computing units self-organizes to implement the desired behavior. This is done in some learning algorithms by presenting some examples of the desired input-output mapping to the network.

A correction step is executed iteratively until the network learns to produce the desired response. The learning algorithm is a closed loop of presentation of examples and of corrections to the network parameters as below:

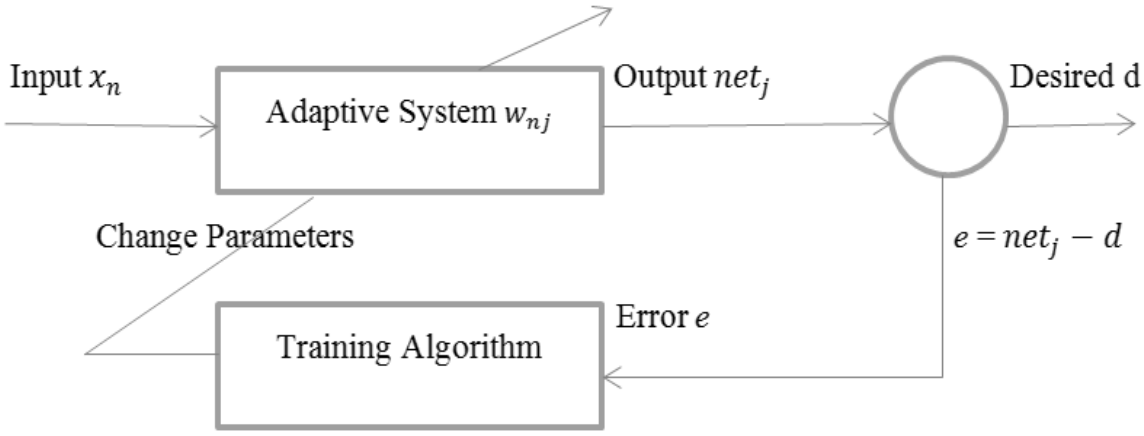

Figure 2.6: Closed Loop ANN learning

Let $w_{nj}(n)$ denote the value of the synaptic weight w_{nj} at time n. At time n an adjustment $\Delta w_{nj(n)}$ is applied to the synaptic weight $w_{nj}(n)$ yielding the updated value

$$w_{nj}(n+1) = w_{nj}(n) + \Delta w_{nj}(n) \qquad (2.36)$$

A prescribed set of well-defined rules for the solution of a learning problem is called a learning/training algorithm. As expected, there is no unique learning algorithm for the design of neural netroworks. Rather, we, we have a kit of tools represented by a diverse variety of learning algorithms, each of which offers advantages of its own.

Let $d_k(n)$ denote some desired response or target response for neuron k at time n. Let the corresponding value of the actual response (output) of this neuron be denoted by net_j. The response $net_j(n)$ is produced by a stimulus applied to the input of the network

in which neuron *k* is embedded. The input vector and desired response $d_k(n)$ constitute a particular sample presented to the network at time *n*.

Typically, the actual response $net_j(n)$ of neuron *k* is different from the desired response $d_k(n)$.

Hence, we may define an error signal as

$$e_k(n) = net_j(n) - d_k(n) \tag{2.37}$$

The ultimate purpose of error-correction learning is to minimize a cost function based on the error signal $e_k(n)$.

A criteria commonly used for the cost function is the instantaneous value of the mean-square-error criterion.

$$J(n) = \frac{1}{2}\sum_k e_k^2(n) \tag{2.38}$$

The network is then optimized by minimizing $J(n)$ with respect to the synaptic weights of the network. Thus, according to the error-correction learning rule, the synaptic weight adjustment is given by:

$$\Delta w_{kj} = \mu e_k(n) x_j(n) \tag{2.39}$$

Learning can either be supervised, unsupervised or an hybrid of both.

In supervised learning, some input vectors are collected and presented to the network. The output computed by the network is observed and the deviation from the expected answer is measured. The weights are corrected according to the magnitude of the error in the way defined by the learning algorithm as illustrated below;

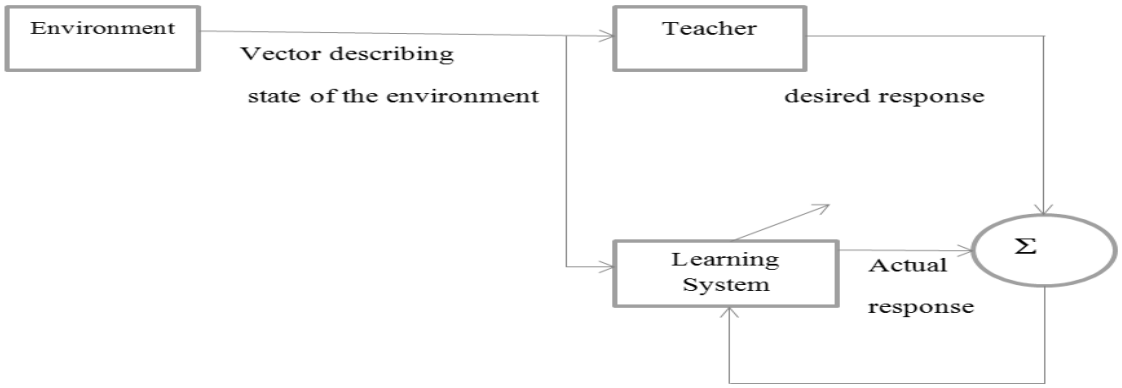

Figure 2.7: ANN Supervised Learning

In unsupervised learning, for a given input, the exact numerical output a network should produce is unknown. i.e. There is no external teacher to oversee the learning process. Provision is made for a task-independent measure of the quality of representation that the network is required to learn and the free parameters of the network are optimized with respect to that measure.

Once the network has become tuned to the statistical regularities of the input data, it develops the ability to form internal representations for encoding features of the input and thereby creates new classes automatically. This is illustrated below:

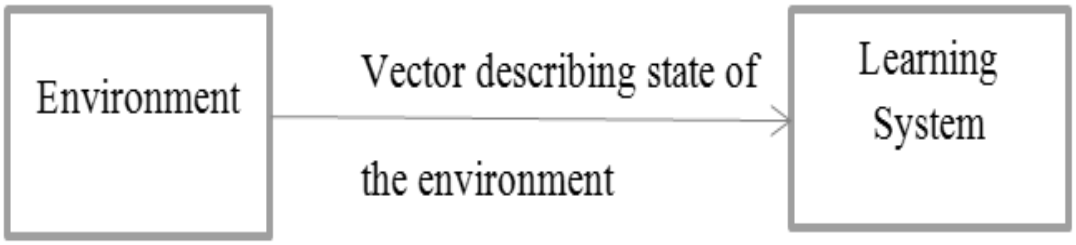

Figure 2.8: ANN Unsupervised Learning

Neural networks are often used for statistical analysis and data modelling in which their role is perceived as an alternative to standard nonlinear regression or cluster analysis techniques. They are used in problems that may be couched in terms of classification or forecasting.

The first stage of model predictive control is to train a neural network to represent the forward dynamics of the plant. The prediction error between the plant output and the neural network output is used as the neural network training signal. The process is represented by the following figure:

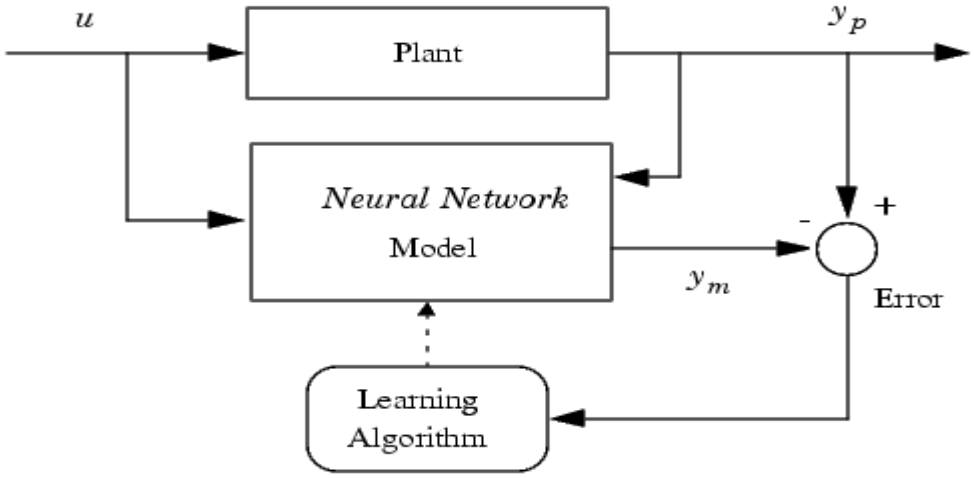

Figure 2.9: ANN Training Model

This network can be trained offline in batch mode, using data collected from the operation of the plant. One can use any of the training algorithms in Backpropagation for network training.

2.4 Cost-Benefit Analysis Techniques

There are various appraisal techniques used to evaluate possible investment opportunities and to determine which of these opportunities will generate the best returns. These techniques are broadly classified into two, namely the Non-discounted cash flow Methods and the discounted cash flows Methods (Choudhurry, 1988; Co. E. I., 2000; Incose, 2006; Dutta, 2009; Kerzner, 2009).

Under Non-discounted Methods we have the Payback Period, Accounting Rate of Return and the Debt Service Coverage Ratio.

The payback period is the length of time required to recover the initial cost of an investment. The payback period of a given investment is an important determinant of whether to undertake the project or not. It is computed as:

$$\text{Payback Period} = \frac{\text{cost of Project}}{\text{annual cash inflows}} \tag{2.40}$$

There are three main drawbacks with the payback period method, namely it ignores any benefits that occur after the payback period, it does not account for the time value of money and that it does not account for asset depreciation.

The accounting rate of return (ARR) is computed as:

$$\text{ARR} = \frac{\text{average annual net inflows} - \text{annual depreciation}}{\text{net investment outlay}} \tag{2.41}$$

There are several challenges with the accounting rate of return concept namely it does not factor the time value of money and it is not an adequate measure of comparing one project to another.

The Debt-Service Coverage Ratio (DSCR) is a measure of the cash flow available to pay current debt obligations defined as:

$$\text{DSCR} = \frac{\text{net profit} + \text{interest (on long term loan)} + \text{depreciation}}{\text{interest (on long term loan)} + \text{principal loan}} \tag{2.42}$$

A DSCR greater than one means the entity has sufficient income to pay its current debt obligations. The Debt Service Coverage Ratio is very important from the lender's point of view. It indicates the number of times interest is covered by the profits available to pay interest charges. A high debt service ratio or interest coverage ratio assures the lender of a regular and periodic interest income.

In Discounted cash flows Methods we have Net Present Value, Benefits Cost ratio and the Internal rate of return.

Net present value (NPV) is the present value of net cash inflows generated by a project including salvage value, if any, less the initial investment on the project. It is the difference between the present value of cash inflows and the present value of cash outflows computed as:

$$NPV = \sum_{t=0}^{n} \frac{C_t}{(1+r)^t} \qquad (2.43)$$

Where t = time for cash flow**,** n = the total time of the project, r = discount rate and *C*t = the net cash flow at time t (the difference between benefits and costs).

A positive net present value indicates that the projected earnings generated by an investment exceed the anticipated costs. Generally, an investment with a positive NPV will be a profitable one and one with a negative NPV will result in a net loss (Kerzner, 2009).

The discount rate used is the weighted average cost of capital-cost of borrowing money from banks and other institutions plus a risk factor to take care of inflation, repair and

maintenance costs and other uncertainties. It is a way to account for the time value of money.

One primary issue with gauging an investment's profitability with NPV is that NPV relies heavily upon multiple assumptions and estimates, so there can be substantial room for error. Estimated factors include investment costs, discount rate and projected returns. A project may often require unforeseen expenditures to get off the ground or may require additional expenditure at the project's end.

Additionally, discount rates and cash inflow estimates may not inherently account for risk associated with the project and may assume the maximum possible cash inflows over an investment period. This may occur as a means of artificially increasing investor confidence.

Another difficulty with using NPV alone is that risk is assumed to be equal among competing projects. Risk is seldom equal in practice. Portfolio diversification is an acknowledged risk reduction technique. Similarly several smaller projects should have less risk than one large one, all other things being equal. NPV favors larger projects whereas smaller ones inherently have less risk.

The Internal rate of return (IRR) is the discount rate often used in capital budgeting that makes the net present value of all cash flows from a particular project equal to zero.IRR being a rate of ratio is uniform for investments of varying types and, as such, IRR can be used to rank multiple prospective projects a firm is considering on a relatively even basis.

When using IRR to compare projects of different lengths, there is always a challenge in that a project of a short duration may have a high IRR, making it appear to be an excellent investment, but may also have a low NPV. Conversely, a longer project may have a low IRR, earning returns slowly and steadily, but may add a large amount of value to the company over time.

2.5 Load Flow Solution

Load flow studies are one of the most important aspects of power system planning and operation. It gives us the sinusoidal steady state of the entire system – voltage magnitudes and angles at each bus, real and reactive power generated and absorbed and line losses (University L. , 2009).

The steady state real and reactive powers supplied by a bus in a power network are expressed in terms of nonlinear algebraic equations. We therefore use iterative methods for solving these equations**.** Let the voltage at the i^{th} bus be denoted by;

$$V_i = |V_i| \angle \delta_i = |V_i| (\cos \delta_i + j \sin \delta_i) \tag{2.44}$$

Also let the self-admittance at bus *i* be:

$$Y_{ii} = |Y_{ii}| \angle \theta_{ii} = |Y_{ii}| (\cos \theta_{ii} + j \sin \theta_{ii}) = G_{ii} + jB_{ii} \tag{2.45}$$

Similarly the mutual admittance between the buses *i* and *j* can be written as

$$Y_{ij} = |Y_{ij}| \angle \theta_{ij} = |Y_{ij}| (\cos \theta_{ij} + j \sin \theta_{ij}) = G_{ij} + jB_{ij} \tag{2.46}$$

Let the power system contain a total number of n buses. The current injected at bus i is given as;

$$\begin{aligned} I_i &= Y_{i1}V_1 + Y_{i2}V_2 + \cdots + Y_{in}V_n \\ &= \sum_{k=1}^{n} Y_{ik}V_k \end{aligned} \tag{2.47}$$

It is to be noted we shall assume the current entering a bus to be positive and that leaving the bus to be negative. As a consequence the real and reactive power entering a bus will also be assumed to be positive. The complex power at bus i is then given by;

$$\begin{aligned} P_i - jQ_i = V_i^* I_i &= V_i^* \sum_{k=1}^{n} Y_{ik}V_k \\ &= |V_i|(\cos\delta_i - j\sin\delta_i)\sum_{k=1}^{n}|Y_{ik}V_k|(\cos\theta_{ik} + j\sin\theta_{ik})(\cos\delta_k + j\sin\delta_k) \\ &= \sum_{k=1}^{n}|Y_{ik}V_iV_k|(\cos\delta_i - j\sin\delta_i)(\cos\theta_{ik} + j\sin\theta_{ik})(\cos\delta_k + j\sin\delta_k) \end{aligned} \tag{2.48}$$

Note that

$$\begin{aligned} &(\cos\delta_i - j\sin\delta_i)(\cos\theta_{ik} + j\sin\theta_{ik})(\cos\delta_k + j\sin\delta_k) \\ &\quad = (\cos\delta_i - j\sin\delta_i)[\cos(\theta_{ik} + \delta_k) + j\sin(\theta_{ik} + \delta_k)] \\ &\quad = \cos(\theta_{ik} + \delta_k - \delta_i) + j\sin(\theta_{ik} + \delta_k - \delta_i) \end{aligned} \tag{2.49}$$

Therefore substituting in (2.49) we get the real and reactive power as

$$P_i = \sum_{k=1}^{n} \left| Y_{ik} V_i V_k \right| \cos\left(\theta_{ik} + \delta_k - \delta_i\right) \tag{2.50}$$

$$Q_i = -\sum_{k=1}^{n} \left| Y_{ik} V_i V_k \right| \sin\left(\theta_{ik} + \delta_k - \delta_i\right) \tag{2.51}$$

The main objective of the load flow is to find the voltage magnitude of each bus and its angle when the powers generated and loads are pre-specified. To facilitate this we classify the different buses of the power system as:

- Load (P-Q) Buses: In these buses no generators are connected and hence the generated real power P_{Gi} and reactive power Q_{Gi} are taken as zero. The load drawn by these buses are defined by real power $-P_{Li}$ and reactive power $-Q_{Li}$ in which the negative sign accommodates for the power flowing out of the bus.
- Voltage Controlled (P-V) Buses: These are the buses where generators are connected. The power generation in such buses is controlled through a prime mover while the terminal voltage is controlled through the generator excitation. Keeping the input power constant through turbine-governor control and keeping the bus voltage constant using automatic voltage regulator, we can specify constant $P_{G.}$
- Slack (Swing) Bus: This bus sets the angular reference for all the other buses against which angles of all the other bus voltages are measured. For this reason

the angle of this bus is usually chosen as 0°. Furthermore it is assumed that the magnitude of the voltage of this bus is known.

Let real and reactive power generated at bus i be denoted by P_{Gi} and Q_{Gi} respectively. Also let us denote the real and reactive power consumed at the i^{th} bus by P_{Li} and Q_{Li} respectively. Then the net real power injected at bus i is

$$P_{i,inj} = P_{Gi} - P_{Li} \tag{2.52}$$

Let the injected power calculated by the load flow program be $P_{i,calc}$. Then the mismatch between the actual injected and calculated values is given by

$$\Delta P_i = P_{i,inj} - P_{i,calc} = P_{Gi} - P_{Li} - P_{i,calc} \tag{2.53}$$

In a similar way the mismatch between the reactive power injected and calculated values is given by

$$\Delta Q_i = Q_{i,inj} - Q_{i,calc} = Q_{Gi} - Q_{Li} - Q_{i,calc} \tag{2.54}$$

The purpose of the load flow is to minimize the above two mismatches. It is to be noted that (2.50) and (2.51) are used for the calculation of real and reactive power in (2.53) and (2.54).

However since the magnitudes of all the voltages and their angles are not known a priori, an iterative procedure must be used to estimate the bus voltages and their angles in order to calculate the mismatches.

It is expected that mismatches ΔP_i and ΔQ_i reduce with each iteration and the load flow is said to have converged when the mismatches of all the buses become less than a very small number.

Gauss-Seidel and Newton-Raphson are common iteration techniques used in many power flow software including MATLAB.

2.6 Current Research Trends in the use of Facts Devices in Voltage Stability Improvement

In reference (Gupta, 2010) a 5-Bus, 2-Generator 500/230kV looped power system model was used to demonstrate the use of UPFC as a power flow control device. The model showed that UPFC can help in power flow control, faster steady state achievement and an improved voltage profile.

In reference (Boon, 2009) the use of UPFC for voltage stability improvement using Alternative Transients Program/Electromagnetic Transients Program-ATP/EMTP software on the Thailand transmission system was researched on.

In references (Anathapadmanabha, 2006) and (Reddy, 2012) transmission loss minimization on a IEEE 30-Bus system for several loading conditions was simulated. The UPFC devices were installed on the system depending on the voltage stability index, voltage change index and active power loss sensitivity factors computed after doing the load flow solution.

A loss minimization study was performed on the IEEE 9-Bus and 14-Bus systems using Power System Analysis Toolbox-PSAT software in reference (P.Vijayarpiya, 2010).The optimal UPFC location was done using different power flow analyses techniques such as small signal analysis, hopf bifurcation and time domain analysis. The loadability increased from 17.5% to 41.89% for the 14-bus system.

A research on voltage stability and loss reduction by using the voltage stability index to locate the best UPFC location and using genetic algorithm and particle swarm optimization for the UPFC control was done on reference (Kumar, 2011).

In references Reddy (2012) and Tulasiram (2008) Simulation of real and reactive power flow control with UPFC connected to a transmission line, the real and reactive power flow control through a transmission line by placing UPFC at the sending end of the line was studied. The UPFC control was done using pulse width modulation so as to generate firing pulses for the two converters. Using PSCAD software, it was shown that there was an improvement of real and reactive power flow through the transmission line.

In reference (Anathapadmanabha, 2011) an optimal UPFC location study under line outage contingencies using fuzzy approach to combine the effects of voltage stability margin indicated by minimum singular value of the load flow jacobian matrix and voltage change was done.

A Newton-Raphson based load flow calculation program through which control settings of UPFC can be determined directly was developed in references (Chengaiah, 2012) and (Poornachandrarao, 2012).This was done by keeping the N-R load flow algorithm intact

and required only some modification of the jacobian matrix in the MATLAB iterations so as to achieve convergence. Using Matlab, the control settings of UPFC for different pre-specified power flows for IEEE 14-bus system were obtained.

An assessment of the optimal UPFC location using P-V curves by considering steady-state voltage stability on a 7-machine, 23-bus test system was done in reference (Yokohama, 2009).

In (Rani, 2012) the use of UPFC for the enhancement of power flow over a 5-Bus 500KV transmission system using MATLAB was done. The performance of UPFC under dynamic load conditions as well as during fault conditions were studied. The results indicated the usefulness of the UPFC in improving transient stability, voltage profile, power flow control and faster steady state achievement.

In references Singh (2012) unified the power flow controller optimal power flow model, Muthukrishnana (2010) and Ajami (2007) a two machine test system was simulated on Matlab to show that the UPFC has the capability to control the line active and reactive power flows in steady state and transient conditions.

Finally, in (Renz, 1999) a commissioning study of the UPFC installed at the Inez substation of American Electric Power in Eastern Kentucky to increase power transfer capability and provide voltage support in the area was done. The tests showed that the UPFC was able to do control of real power flow, reactive power control and improvement in voltage stability.

This research work sought to advance the current knowledge on voltage stability improvement and loss reduction by using the voltage stability indices to get the best UPFC location and replacement of a human system operator for real time control using ANN. The work was done on a much bigger system-the IEEE 39-Bus system- and PSAT on Simulink environment which has not been done before.

CHAPTER THREE

METHODOLOGY

3.1 The Developed System

This research work had four specific objectives. It began with a voltage-security constrained load flow analysis on the 39-Bus IEEE test system followed by the optimal placement of the UPFC using voltage stability indices. After this an artificial neural networks system was developed to instruct the UPFC to either inject or absorb reactive power accordingly. Finally, a cost-benefit analysis of the developed system was done. This is summarized in the block diagram below;

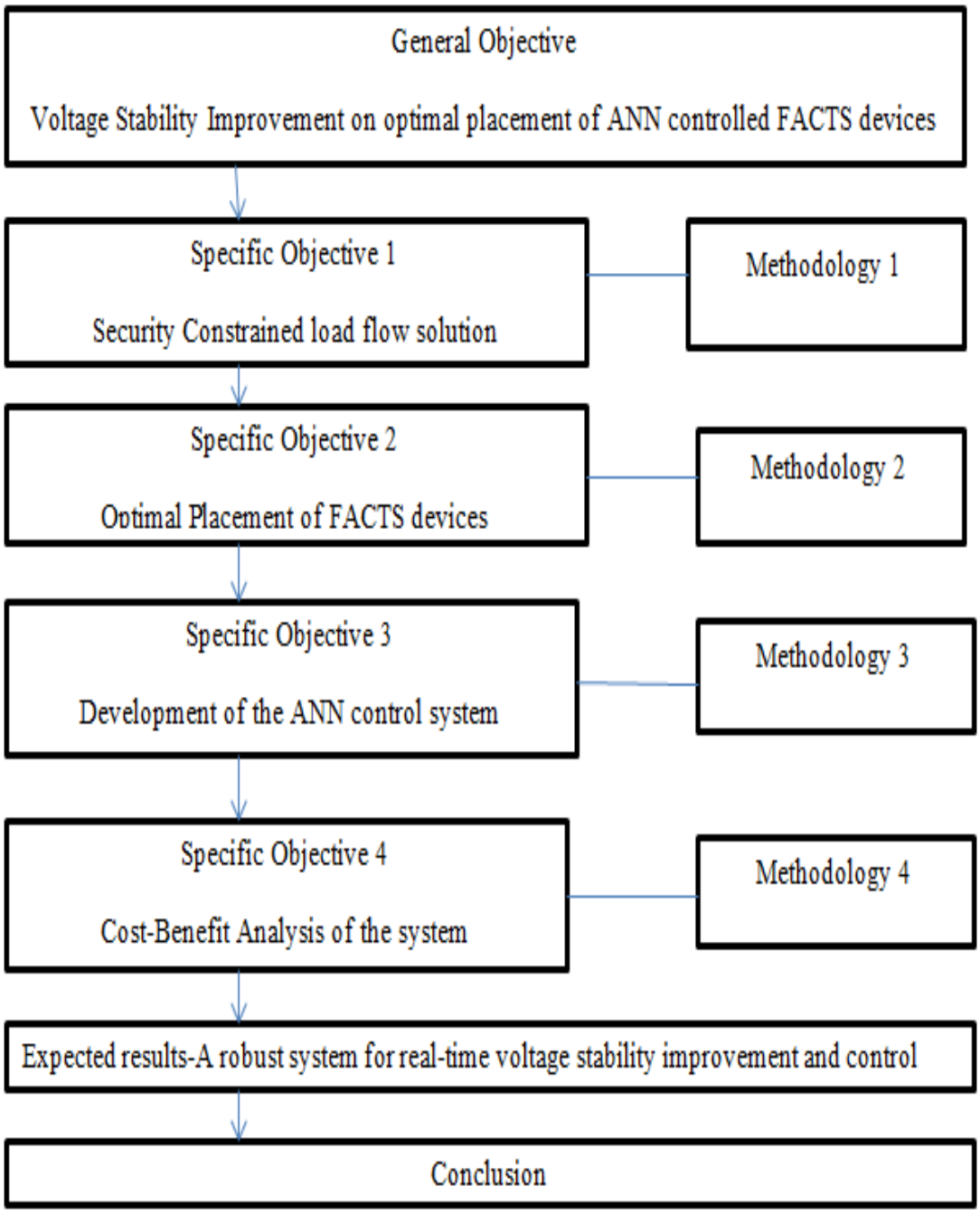

Figure 3.1: Flow of the methodology

At the end of the research work, the developed system was as summarized in the diagram below:

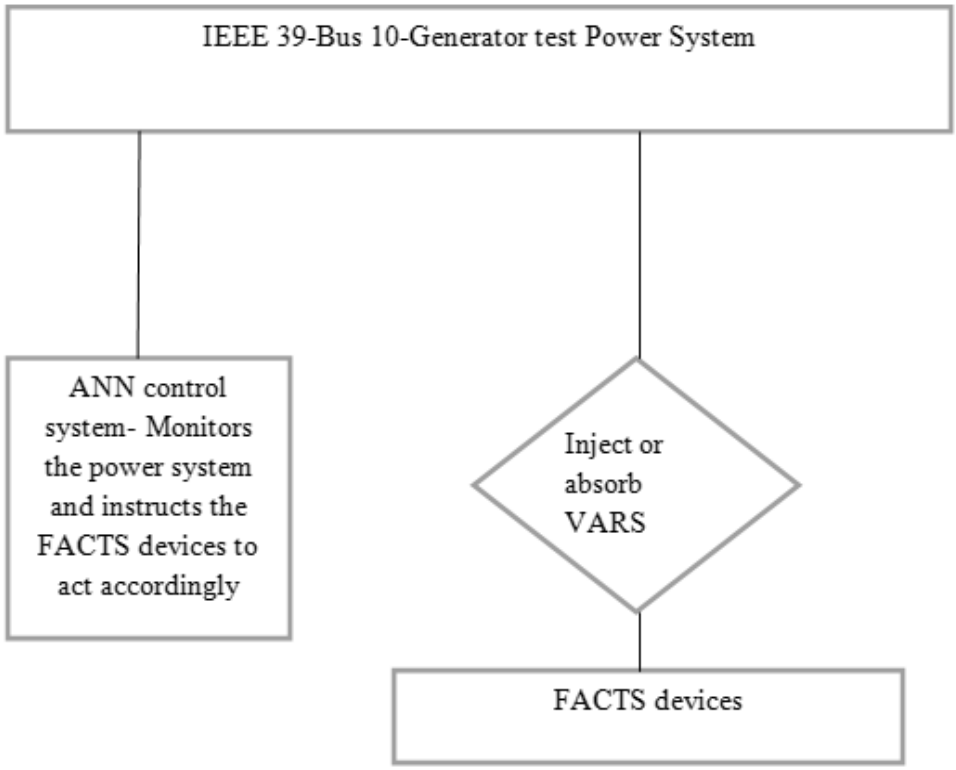

Figure 3.2: Research Block diagram

3.2 Load Flow Solution

A voltage-security constrained optimal load flow solution was carried out on a base of 100MVA using data in Appendix A1 as the base case. The constraints were capping of the voltage profile to 1.0 per unit and minimization of reactive power losses for better voltage stability. The 39-Bus test system was initially modelled in Matlab's Simulink toolbox as per the data in appendix A1.After that, a load flow was carried out in PSAT toolbox.

This was key in modelling the nonlinear relationships among bus power injections, power demands and bus voltages and angles with the network constants providing the various circuit parameters as the appendix A1.

The main information of load flow analysis was to find the magnitude and phase angle of voltage at each bus and the real and reactive power flowing in each transmission line. This formed the basis of the voltage stability indices that were used to optimally locate the UPFC.

3.3 Optimal Placement of Facts Devices

The voltage security-constrained load flow solution above formed the basis of determining the optimal location of the UPFC. The devices were optimally located such that they have the greatest positive impact towards voltage stability of the entire network. This was determined by using a ranking system of the voltage stability indices such that buses exhibiting low voltages were candidates for location of FACTS devices provided that they satisfied the set load flow constraints. PSAT Software was used to find the voltage stability indices of the load buses by selecting one bus at a time.

The Voltage Stability Indices-Fast Voltage Stability Index and the Line Stability Index-were computed by increasing the reactive power gradually at a chosen load bus until the load flow solution fails to give result while keeping the real power constant. That is, it reaches the instability point.

At this instability point, the connected load at the particular bus was determined as the maximum loadability. The maximum loadability for every load bus were sorted in ascending order with smallest value being ranked highest for all the 19 load buses.

The ranking was done using equations (2.28) and (2.31) for FVSI and LSI respectively. The highest rank implies the weakest bus in the system that has the lowest sustainable load.

3.4 Ann Control System

The UPFC model used was as shown below

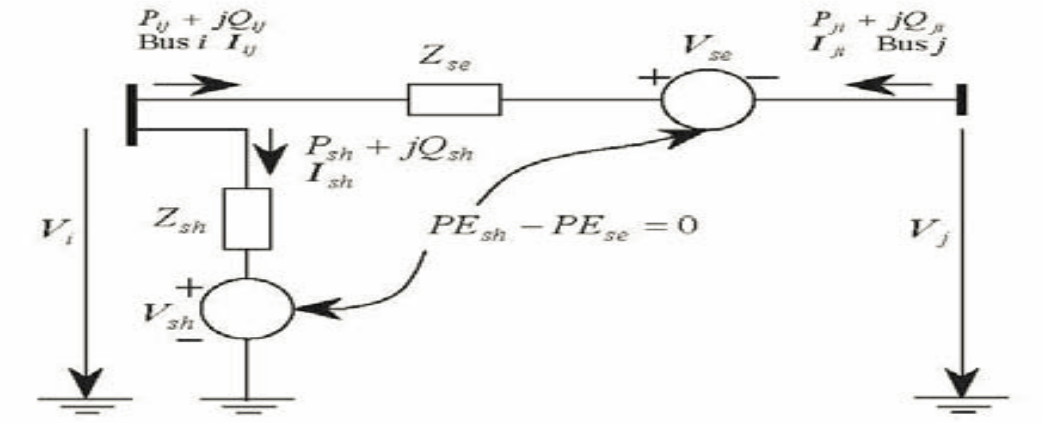

Figure 3.3: UPFC Model used for the control strategy

In the above model, given that

$V_{sh} = V_{sh} < \theta_{sh}, V_{se} = V_{se} < \theta_{se}, V_i = V_i < \theta_i, V_j = V_j < \theta_j$, then the power flow constraints of the UPFC shunt and series branches from (2.18) and (2.19)

$$P_{sh} = V_i^2 g_{sh} - V_i V_{sh} \{ g_{sh} \cos(\theta_i - \theta_{sh}) + b_{sh} \sin(\theta_i - \theta_{sh}) \} \quad (3.1)$$

$$Q_{sh} = -V_i^2 b_{sh} - V_i V_{sh} \{ g_{sh} \sin(\theta_i - \theta_{sh}) - b_{sh} \cos(\theta_i - \theta_{sh}) \} \quad (3.2)$$

$$P_{ij} = V_i^2 g_{ij} - V_i V_j (g_{ij} \cos\theta_{ij} + b_{ij} \sin\theta_{ij}) - V_i V_{se} \{ g_{ij} \cos(\theta_i - \theta_{se}) + b_{ij} \sin(\theta_i - \theta_{se}) \} \quad (3.3)$$

$$Q_{ij} = -V_i^2 b_{ij} - V_i V_j (g_{ij} \sin\theta_{ij} - b_{ij} \cos\theta_{ij}) - V_i V_{se} \{ g_{ij} \sin(\theta_i - \theta_{se}) - b_{ij} \cos(\theta_i - \theta_{se}) \} \quad (3.4)$$

$$P_{ji} = V_j^2 g_{ij} - V_i V_j (g_{ij} \cos\theta_{ji} + b_{ij} \sin\theta_{ji}) + V_j V_{se} \{ g_{ij} \cos(\theta_j - \theta_{se}) + b_{ij} \sin(\theta_j - \theta_{se}) \} \quad (3.5)$$

$$Q_{ji} = -V_j^2 b_{ij} - V_i V_j (g_{ij} \sin\theta_{ji} - b_{ij} \cos\theta_{ji}) + V_j V_{se} \{ g_{ij} \sin(\theta_j - \theta_{se}) - b_{ij} \cos(\theta_j - \theta_{se}) \} \quad (3.6)$$

$$where\ g_{sh} + jb_{sh} = 1/Z_{sh},\ g_{ij} + jb_{ij} = 1/Z_{se},\ \theta_{ij} = \theta_i - \theta_j, \theta_{ji} = \theta_j - \theta_i$$

The shunt and series active and reactive power was absorbed/supplied as per the above equations continuously solved using iterative techniques.

A UPFC control system using artificial neural networks was developed in Matlab's neural networks toolbox. The system was trained so that it can control the UPFC in its generation and absorption of reactive power in real time so as to maintain the voltage level to 1.0 per unit.

In this research, the ANN had three inputs namely, the difference between the measured real power and its reference value, the difference between the measured reactive power and its reference value, and the difference between the measured shunt voltage and its reference value, all being continuously monitored for all the buses in the system. The first step was system identification after which the plant model was used by the Neural Network predictive controller to predict future performance.

The first stage of model predictive control was to train a neural network to represent the forward dynamics of the plant. The prediction error between the plant output and the neural network output was used as the neural network training signal as shown below:

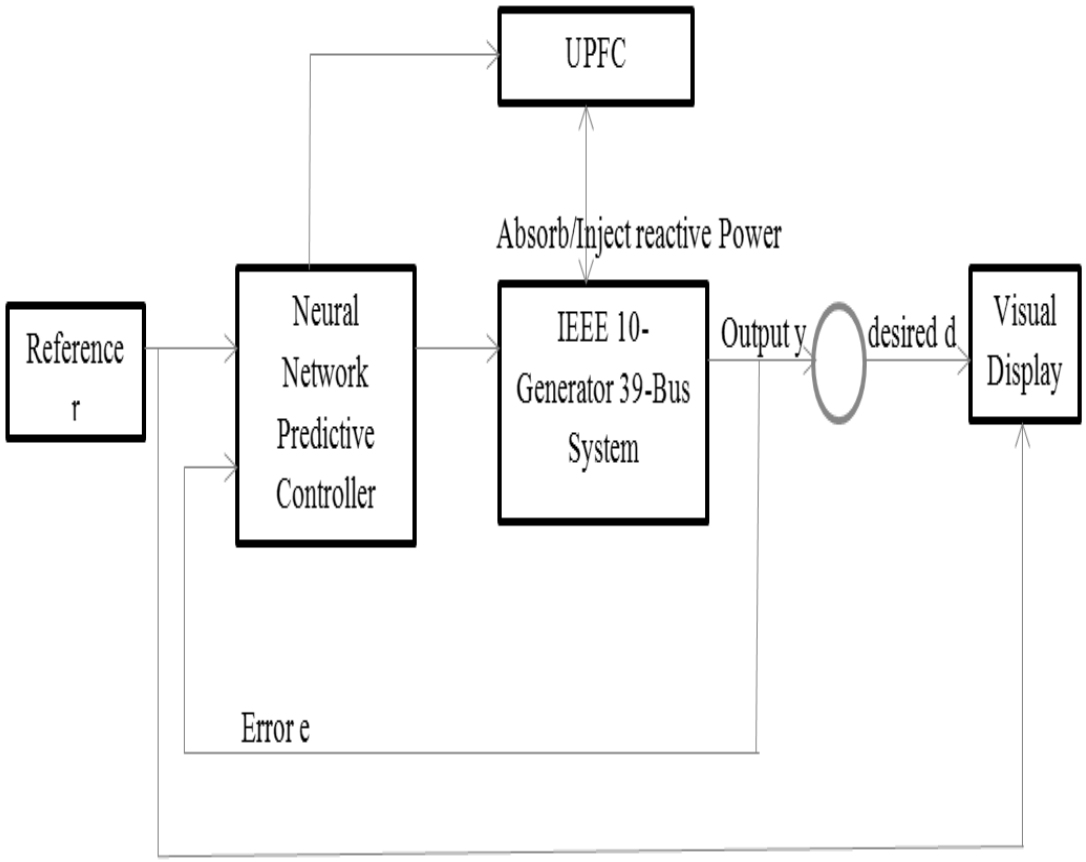

Figure 3.4: ANN Control system Block Diagram

In this case,the reference signal r was the same as the desired output d which was 1.0 per unit voltage.The error signal was e = output y.Using e and r ,the Neural Networks(NN) predictive controller was trained to give the UPFC various commands to either absorb or inject VARS so as to stabilize the voltage level as close to 1.0 per unit as possible.

A set of 4,000 training data was used for the same so that the NN controller can predict future behaviour(in this case,instructions) to the UPFC based on the learned attributes.In our case, the training data comprised of various bus snap voltages during the static load flow solution above.

Our network had 39 output nodes and 4,000 training data and given that a single output node in response to a single training pattern is in error with the mean training error having a maximum value of 1.

For large values of output nodes and training data sets,the single bit-error stopping criterion was satisfied. In our case, the 4,000 data sample was sufficient enough to satisfy the holt-winters forecasting technique set stopping criteria of halting when the rate of change of the error is sufficiently small.

The holt-winters forecasting technique is based on four equations as:

$$
\begin{aligned}
F_t &= \alpha \frac{x_t}{S_{t-k}} + (1-\alpha)(F_{t-1} + T_{t-1}) \\
T_t &= \beta(F_t - F_{t-1}) + (1-\beta)T_{t-1} \\
S_t &= \gamma \frac{x_t}{F_t} + (1-\gamma)S_{t-k} \\
\hat{x_t} &= (F_{t-1} + T_{t-1})S_{t-k}
\end{aligned}
\qquad (3.7)
$$

Where F_t, S_t and T_t denote the smoothing, general trend and long range estimates, *k* the long range period and α,β and γ as voltage, reactive power and active power respectively, which are the model parameters set by trial and error procedures during the actual system training.

3.5 Cost Benefit Analysis of The Developed System

After optimal location, sizing of the UPFC and development of a control system, we did a cost benefit analysis of the developed system using both discounted and non-discounted techniques. The UPFC sizing was done to maximize on voltage security as well as system economy by way of trial and error starting with the small value of 10MVA and progressing upwards.

Under Non-discounted Methods we used the Payback Period and the Debt Service Coverage Ratio to gauge the financial viability of investing in the developed system. In Discounted cash flows Methods we used the Net Present Value to gauge the project viability.

CHAPTER FOUR

RESULTS, ANALYSIS AND DISCUSSION

4.1 Results Obtained

The voltage-security load flow solution was carried out as the base case for this research work. This was done on the IEEE 39-Bus, 10-Generator test system shown in Appendix A1.The load flow converged in 0.388 seconds as shown below;

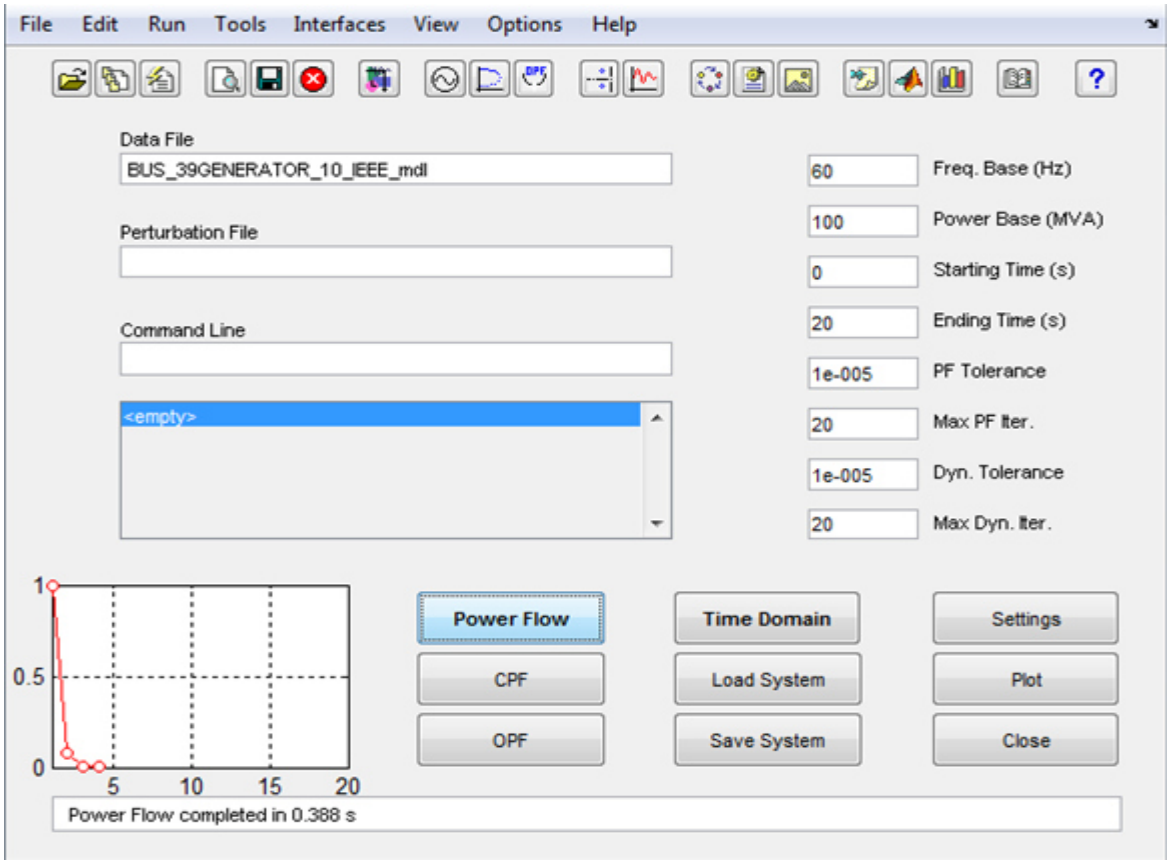

Figure 4.1: Load Flow results convergence (base case)

Using (2.28) and (2.31), a ranking system was developed to determine the stressed and most heavily loaded load buses. The results were as per the table below;

Table 4.1: Maximum reactive power loadability, FVSI and LSI ranking table

RANK	LOAD BUS	FVSI	LSI	LOADABILITY(KVAR)
1	4	0.9224	0.9429	12.5
2	3	0.9125	0.9401	15.4
3	7	0.9115	0.9385	17.5
4	8	0.9075	0.9276	21.9
5	16	0.9029	0.9165	22.6
6	18	0.9009	0.9111	22.8
7	15	0.8997	0.9008	24.8
8	20	0.8901	0.8997	26.5
9	21	0.8899	0.8966	27.7
10	12	0.8865	0.8911	29.2
11	24	0.8725	0.8895	31.1
12	39	0.8711	0.8856	32.1
13	25	0.8615	0.8735	32.4
14	26	0.8556	0.8662	33.2
15	27	0.8433	0.8595	34.5
16	31	0.8256	0.8487	35.7
17	28	0.8166	0.8345	35.9
18	23	0.8127	0.8276	36.5
19	29	0.8066	0.8215	36.8

The table also has the maximum reactive power loadability figures for the various load buses. Load bus#4 was determined as the most heavily stressed and the best candidate for the placement of the UPFC.

Using the bus to bus impedance and reactance values and (2.28) and (2.31) respectively, the UPFC device should be placed on the line connecting bus#4 and bus#14 for maximum impact on voltage stability.

The UPFC device was placed in bus#4 and its value increased progressively from 10MVA with each time a load flow solution being done until an optimal rating of 100MVA was settled on while taking care of the twin objectives of system voltage security and economy. Bigger UPFC values will improve on voltage security but will make the system overly expensive.

On installation of the 100MVA UPFC in load bus #4 between lines 4 and 14, the load flow solution converged in 0.483 as shown below;

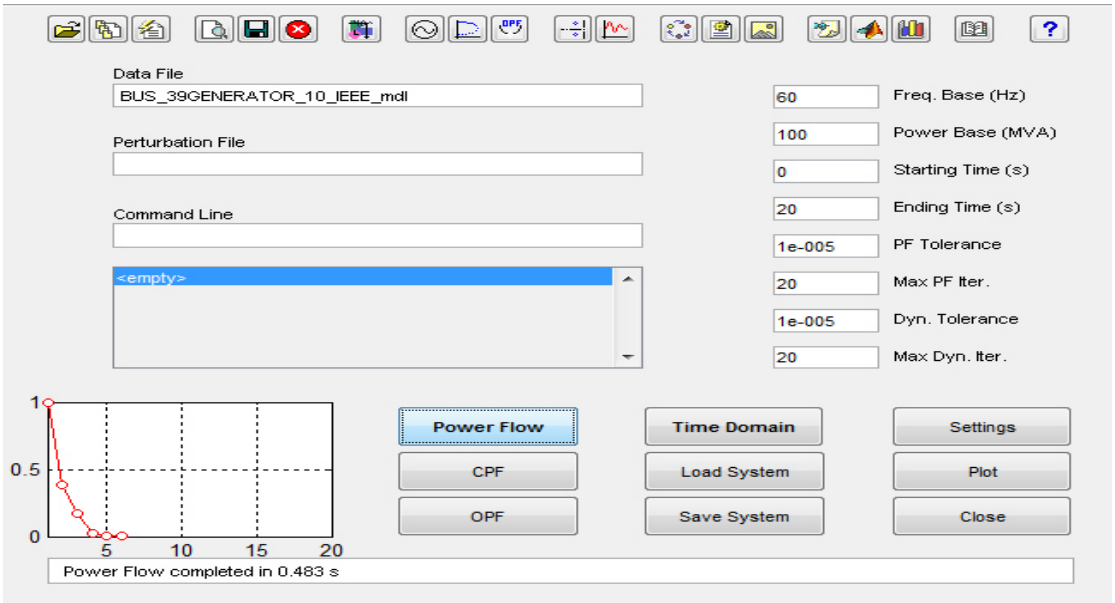

Figure 4.2: Load Flow Solution on UPFC installation convergence

The sparse matrix visualization were as shown below:

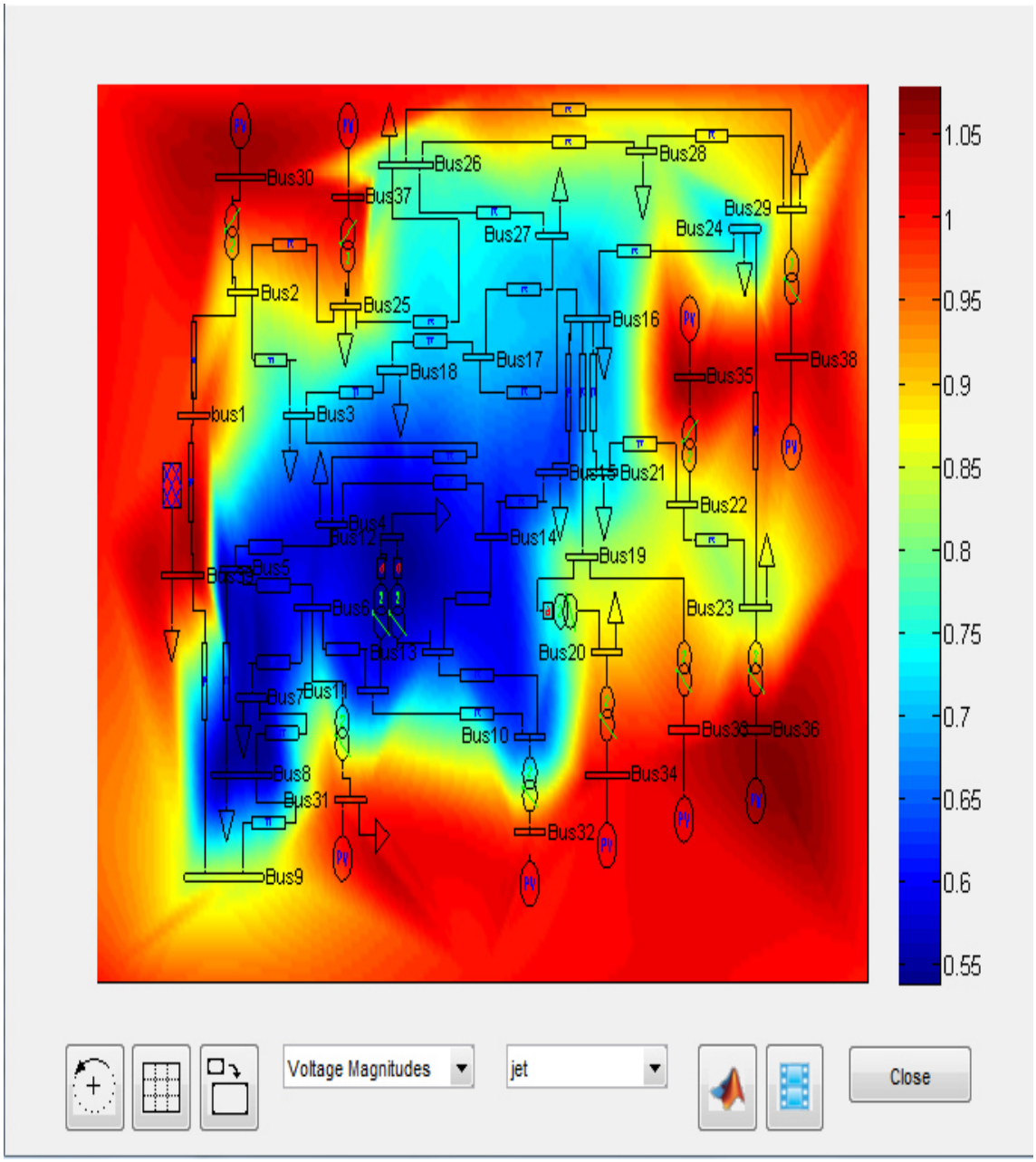

Figure 4.3: Sparse Matrix without UPFC

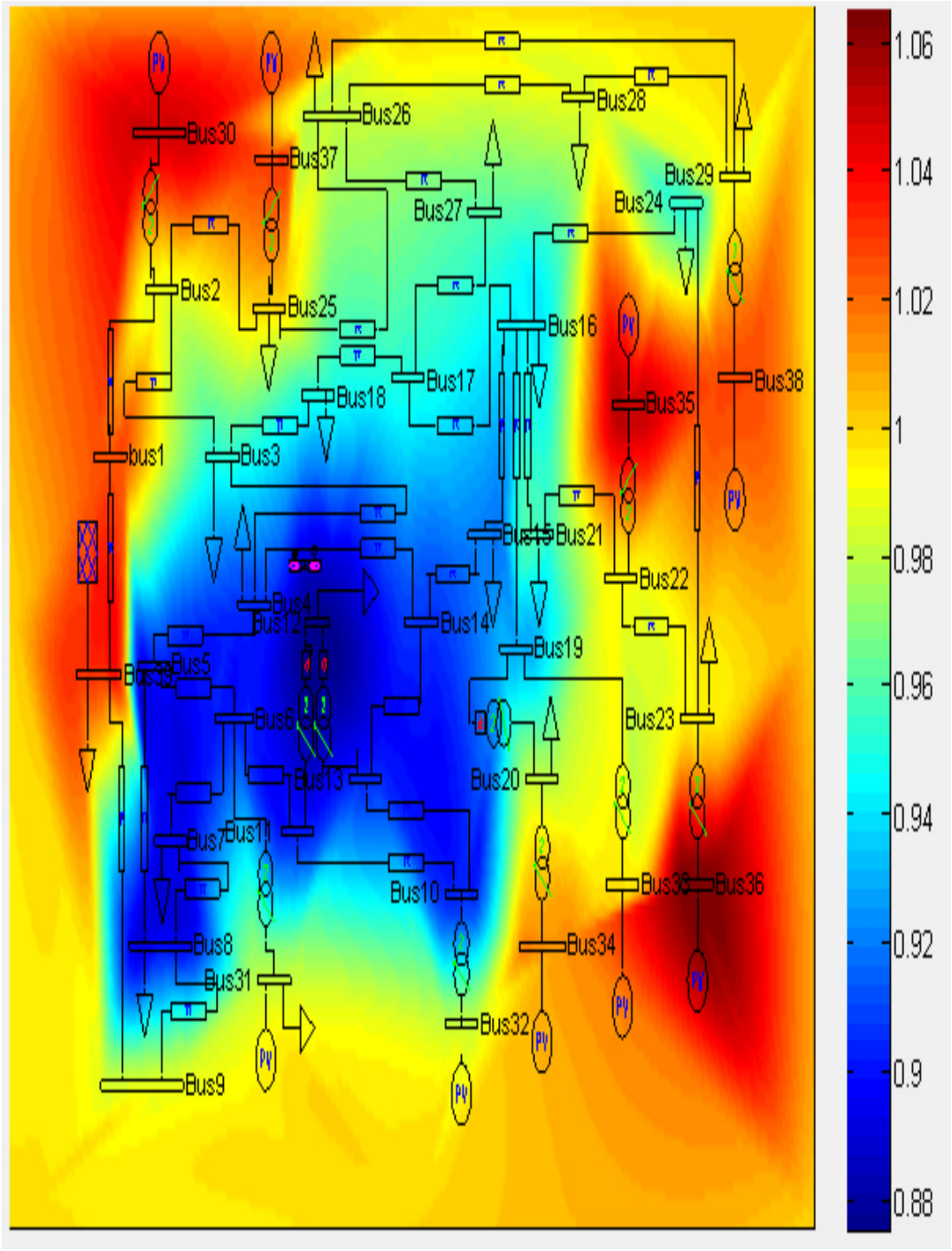

Figure 4.4: Sparse Matrix with UPFC

4.2 Results Analysis and Discussion

There was a slight increase in the load flow convergence time from 0.388 seconds to 0.483 seconds occasioned by the time taken for the UPFC oscillations to settle down. This is traded off by improved voltage profiles as well as active power loss reduction quantified to 1.217MW.

One disadvantage of system variables based VSI used in this research work as opposed to the Jacobian matrix VSI is that they cannot accurately estimate the voltage collapse margin thus they just present critical lines and buses. The latter require a lot of computation time thus not good for online assessment.

The Sparce Matrix visualization figure 4.2 shows a great improvement on voltage profiles on placement of UPFC on load Bus#4.This is corroborated by the improvement of voltage profiles on various buses as per the tables A.3 and A.6.The overall power loss reduction by 1.217MW further attests to the improvement in voltage stability of the system. The loss reduction could have been much higher had the research not been based on a voltage-security constrained test system. This is because of the overly ambitious targeted voltage value of 1.0 per unit (ideal situation) as per the control system developed.

The UPFC location had been done in a way to have maximum impact on the entire network to as to optimize on costs. Buses 7,8 and 12 still did not attain the required minimum voltage level of 1.0 per unit. This should however be viewed in totality in the sense that UPFC has many other benefits that have not been looked at in this research.

These include but not limited to transient stability improvement, dynamic stability improvement, improvement on system dynamic braking and control of mechanically switched capacitors in a power network.

Using a training sample of 4,000 from results obtained from the load flow analysis on installation of the UPFC on the IEEE 39-Bus, 10-Generator test system gave the following results;

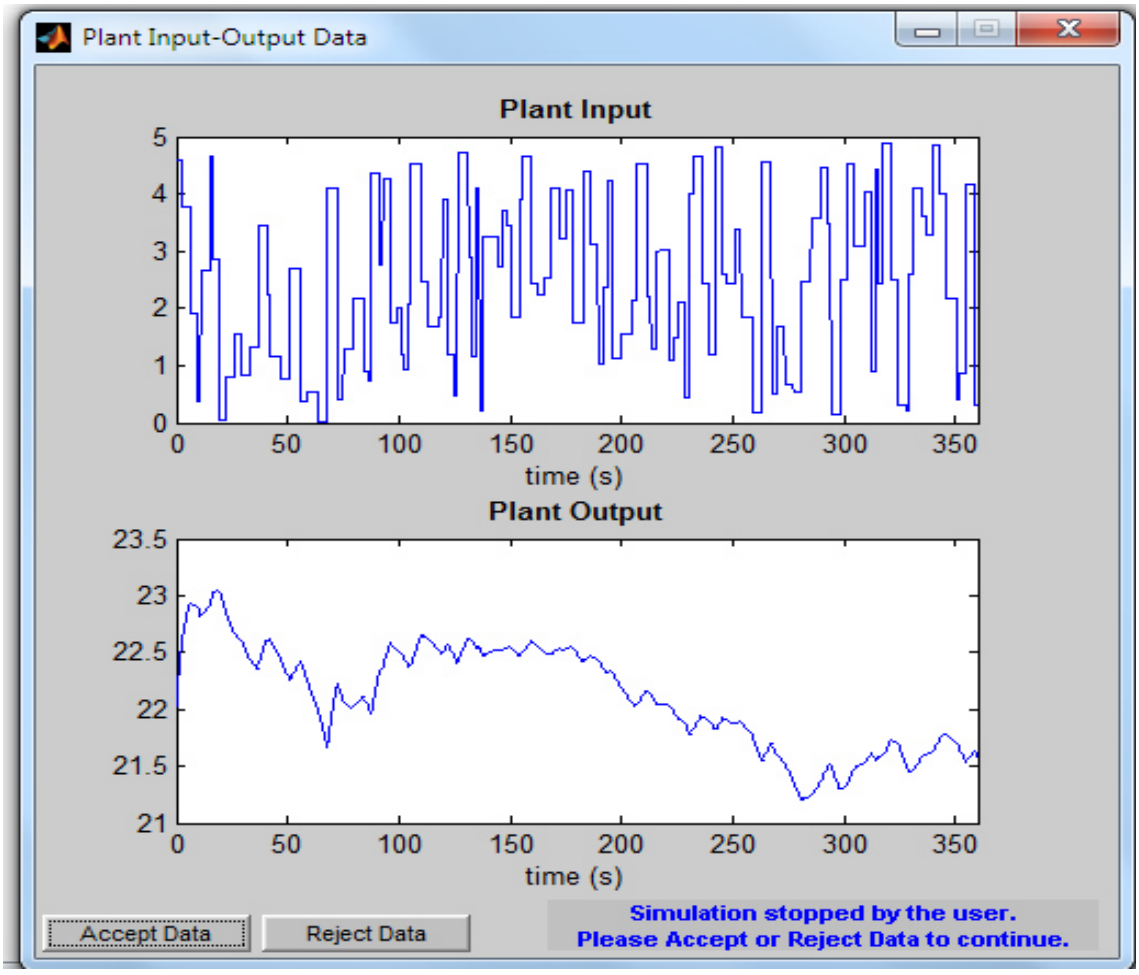

Figure 4.5: ANN Training results

The training results shown above closely mirrored the input data which means that the training data sample used was sufficient. The above output was used to train the Neural Network predictive controller and the results below were obtained;

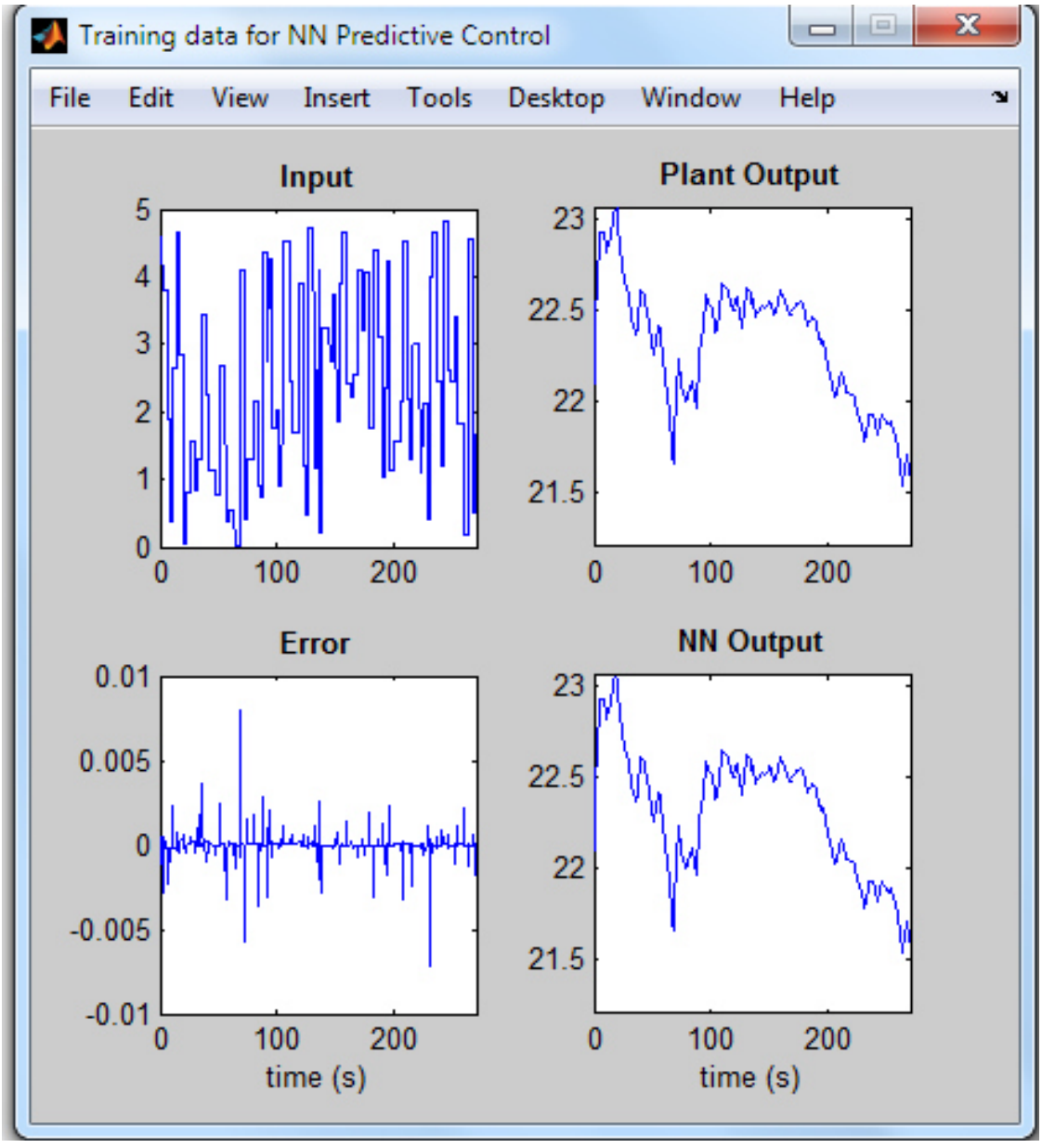

Figure 4.6: Neural Network Predictive Controller Training

The training was finally validated and the results below obtained:

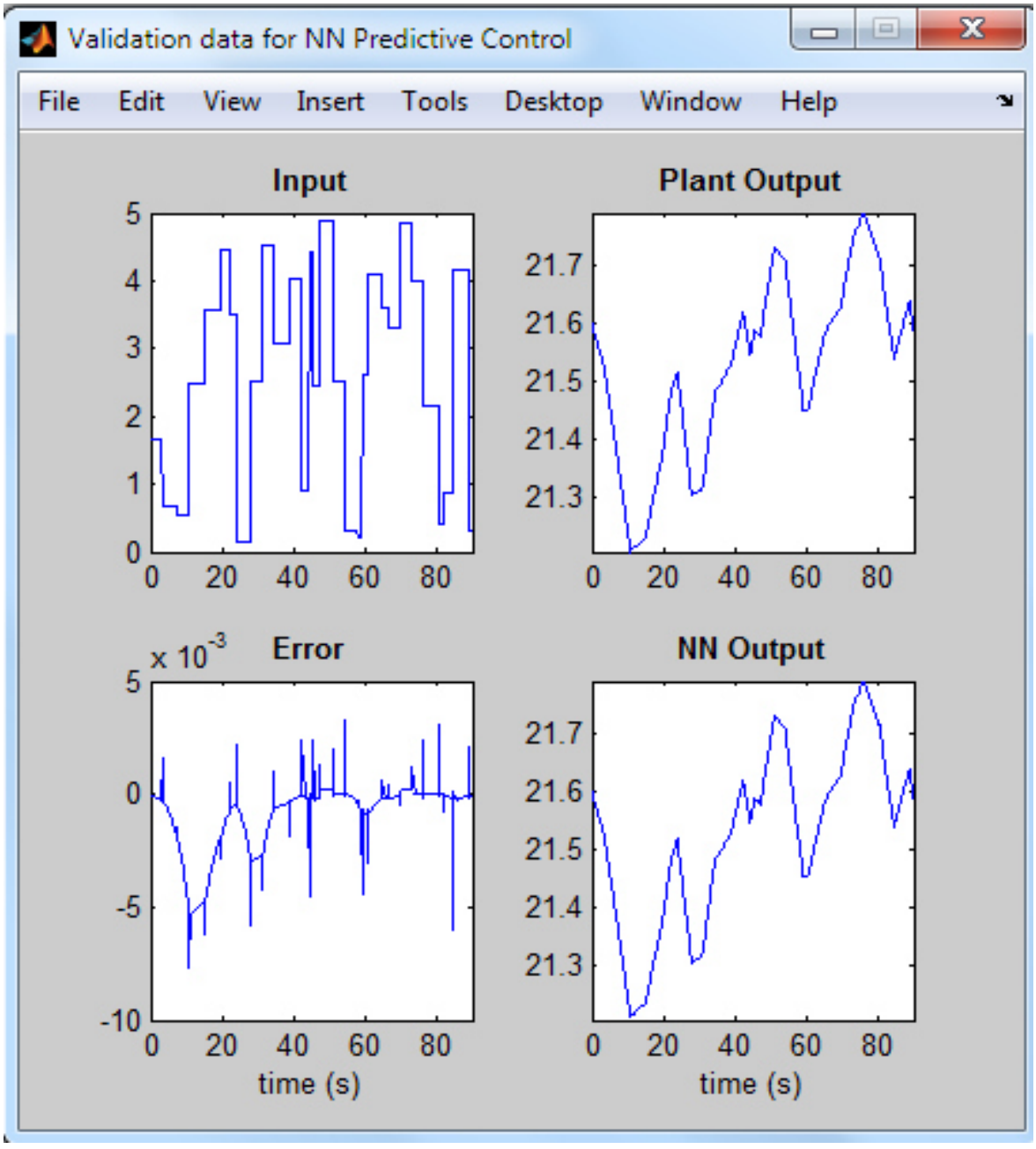

Figure 4.7: ANN Training Validation

The validated results were displayed in a scope's XY graph as shown below:

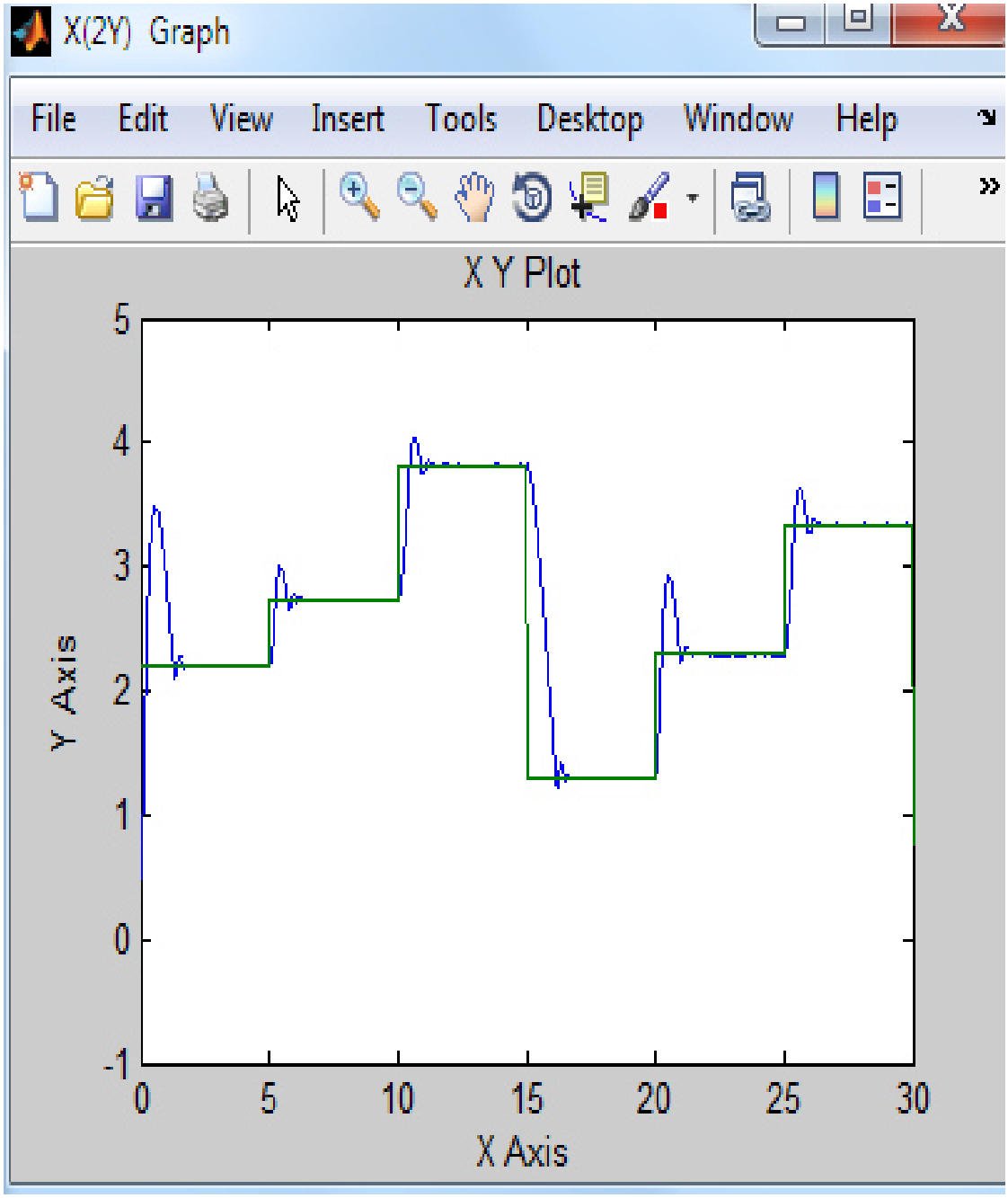

Figure 4.8: ANN Training Validated results display

The green line in figure 4.8 above represents the static values of voltage profiles at various buses and the plus line represents the tracking of the actual bus voltages using an artificial neural networks control system.

The training results above validated against the actual load flow results obtained on the installation of the UPFC indicated that the developed system was a true replica of the training data used which means that it can correctly predict the system behavior and issue correct instructions to the system in future. All this was done using a load factor of 0.8 as per data from Kenya's national power control Kenya. The developed control strategy was tested under various operating conditions such as with a voltage of 0.6,0,7 and 0.8 per unit and in all cases, the validated results were as per figure 4.6 above. In all cases a sample of 4,000 static voltage values were used. The model predictive control method used was based on the receding horizon technique whereby the neural network model predicts the plant response over a specified time horizon.

In our case, we used two sets of instantaneous bus voltage data during load flow analysis for training. One 4,000 data was used as the training set and another 4,000 set of data sample was used as the validation set. The idea was to train the network in the normal way with the training data set but every so often, to do cross-validation with respect to the validation set of data. We stopped training when the validation error reached a minimum error of 0.001 with respect to the validation data set which meant an optimal performance of the neural networks trained system.

In the cost-Benefit Analysis, the UPFC cost is US $60,000 per Million Volt Ampere (MVA) based on information from the Electric Power Research Institute (EPRI) and American Electric Power (AEP) (M.Abed, 1999).

Thus for a 100MVA UPFC, the upfront costs will be as itemized below:

Table 4.2: UPFC Installation Costs

ITEM	**COST(US $)**
100MVA UPFC	6,000,000
System Reinforcements and other accessories	2,000,000
Substation works costs	1,500,000
TOTAL	**9,500,000**

The UPFC leads to a loss reduction of $(0.53442-0.52225)*100=1.217MVA=1.217MW$ at unity power factor. This is computed from the reduction in power loss from the results in tables A.4 and A.7.

For a 15 hours average daily usage as per the data from the national control center daily load profiles, this translates to savings of;

= 1.217*1000*15*30*12 = 6,571,800KWH per annum

In Kenya, the cost of power is US $ 0.2 cents/KWH as per data from the national bureau of statistics of September 2016 thus the annual savings translates to US $1,314,360 (Statistics, 2016).

Thus the project's simple payback period is:

$$\text{Payback period} = \frac{\text{Cost of Project}}{\text{Annual Cash Inflows}} = \frac{9{,}500{,}000}{1{,}314{,}360} = 7.2 \text{ years}$$

To obtain the Debt Service Coverage Ratio (DSCR), we factor in an annual depreciation rate of 8% based on information from the EPRI and AEP and an interest rate of 5% as per international energy projects debt financing models:

Thus the DSCR is:

$$= \frac{\text{net profit} + \text{interest (on long term loan)} + \text{depreciation}}{\text{interest (on long term loan)} + \text{principal loan}}$$

$$- \frac{1{,}314{,}360 + 475{,}000 + 480{,}000}{475{,}000 + 9{,}500{,}000} - 0.23$$

In Discounted cash flows Methods we will use the Net Present Value. With a net cash flow of US $1,314,360 per year equivalent to the savings in terms of system loss reduction.

Assuming that the project is financed by a bank loan payable in ten years with bank interest rates of 5% per annum, a discount rate of 20% will suffice so as to cater for depreciation costs, inflation costs and other unforeseen costs. The rate of inflation at

September 2016 stood at 9.5% as per data from the Kenya National Bureau of Statistics (Statistics, 2016).

Thus year 1 cash inflow will be equal to 1,140,000-1,314,360= US $ 174,315

The annual net cash flow from this project for years 1 to 10 is forecast as follows assuming a 15% increase in utility bills costs every three years and an annual repair and maintenance cost of 2% after the third year: 174,315; 174,315; 174,315; 348,665; 348,665; 348,665;575,380; 575,380; 575,380and 575,380.

The present value (PV) can be calculated for each year as:

At T=0, the present value = -9,500,000 which is the initial investment. The rest are computed as below;

Year	Cash flow	Present value
$T = 1$	$\frac{174{,}315}{(1+0.2)^1}$	= 145,263
$T = 2$	$\frac{174{,}315}{(1+0.2)^2}$	= 121,052
$T = 3$	$\frac{174{,}315}{(1+0.2)^3}$	= 100,877
$T = 4$	$\frac{348{,}665}{(1+0.2)^4}$	= 168,145
$T = 5$	$\frac{348{,}665}{(1+0.2)^5}$	= 140,120
$T = 6$	$\frac{348{,}665}{(1+0.2)^6}$	= 116,767
$T = 7$	$\frac{575{,}380}{(1+0.2)^7}$	= 160,577
$T = 8$	$\frac{575{,}380}{(1+0.2)^8}$	= 133,815
$T = 9$	$\frac{575{,}380}{(1+0.2)^9}$	= 111,512
$T = 10$	$\frac{575{,}380}{(1+0.2)^{10}}$	= 92,927

The sum of all these present values is the net present value, which equals -8,208,945. Since the NPV is less than zero, then this project is not economically viable as an investment.

Data from the Electric Power Research Institute (EPRI) and American Electric Power (AEP) suggests that the lifetime of a UPFC device averages to ten years thus the use of ten years above for the investment appraisal.

This cost-benefit analysis is purely for the purposes of this research work only. There are other numerous benefits of UPFC installation such as provision of dynamic voltage support and control of mechanically-switched capacitors that are generally slow to react during system disturbances among others.

CHAPTER FIVE

CONCLUSION AND RECOMMENDATIONS FOR FUTURE RESEARCH WORK

5.1 Conclusion

A system to monitor and control voltages at various load buses by injection or absorption of reactive power was developed.

Security Constrained load flow analysis was successfully done on the 39-Bus IEEE test system and formed the base case for this research. Using voltage stability indices, the UPFC was optimally placed on load bus number four. A load flow analysis done thereafter indeed confirmed an improvement in the voltage profiles across the test system used. After that, an artificial neural network was trained to help track voltage profiles at various buses and issue instructions accordingly so as to stabilize voltages in an automated way. Finally, a cost-Benefit analysis of the proposed system was done.

5.2 Recommendations for Future Research Work

Going forward, there is need to develop a more flexible voltage stability improvement control system that is more versatile in terms of carrying out mitigation actions such as knocking off certain loads in case of loss of major generation plants, transferring loads to neighboring buses if need be and islanding.

An hybrid system that incorporates several FACTS devices such as the TCSC-IPFC-HVDC B2B combination and a host of artificial intelligence systems such as ANFIS to control power flow in several lines and interconnected power systems simultaneously while resisting cascaded outages is a good research area going forward.

REFERENCES

Abed, M.A. (1999). *Flexible AC Transmission Systems Benefits study,* Retrieved from: http://www.energy.ca.gov

Ajami, A. (2007). Modelling and Controlling of UPFC for power system transient studies. *ECTI Transactions on Electrical Engineering and communication* (pp. 29-35). London: ECTI.

Anathapadmanabha, T.D. S. (2011). Identification of Unified power flow controller location under line outage contigencies. *International Conference on Advances in electronics and power Engineering* (pp. 122-127). New Delhi: Tata Mc Graw Hill.

Anathapadmanabha, T.P.A. (2006). Installation of Unified power flow controller for voltage stability margin enhancement under line outage contingencies. *Iranian Journal of ELectrical and Computer Engineering*, 90-96.

Boon, P. S. (2009). Analysis and Control of UPFC for Voltage Compesation using ATP/EMTP. *Asian Journal on Energy and Environment*, 241-249.

Chengaiah, C.. (2012). Study on effects of UPFC device in electrical transmission system:Power flow assessment. *International Journal of Electrical and Electronics Engineering*, 66-70.

Choudhurry, S. (1988). Estabilishing the project:Scope,time,cost and Perfomance goals. In S.Choudhurry, *Project Management,* (pp. 38-70). New Delhi: Tata Mc Graw Hill.

Co., E. I. (2000). *A guide to the project Management Body of Knowledge,(*2nd ed.). Newton Square: Electronic Imaging Services Co.

Co., P. S. (2012). *Reactive power management and voltage control in North Eastern region.* Dongtieh-Lower Nongrah: Lapalang.

Dutta, B. (2009). Project Planning and Feasibility Studies. In B. Dutta, *Projects:Planning,Analysis,Selection,Implementation and Review,* (pp. 103-128). New Delhi: Tata McGraw Hill.

Gupta, V. (2010). Study and Effects of UPFC and its control system for power flow control and voltage injection in a power system. *Journal of Engineering Science and Technology*, 2558-2566.

Gyugyi, L. N. H. (2000). *Understanding FACTS;Concepts and Technology of Flexible AC Transmission System,* (2nd ed.). New York: IEEE Press.

Incose. (2006). *Incose System Engineering Handbook*. Seattle: Incose.

Kerzner, H. (2009). Project Management Growth:Concepts and Definitions. In H. Kerzner, *Project Management:A systems Approach to Planning Scheduling and Control,* (10th ed.). New York: John Wiley and Sons.

KNBS, (2016). *Economic Survery 2016.* Nairobi: KNBS.

Kulkarni, K. P. (1998). Control Design and Simulation of UPFC. *IEEE*, 1348-1354.

Kumar, K. S. (2011). Improvement of voltage stability and reduction of power losses by optimal placement of UPFC device by using GA and PSO. *International Journal of Engineering science research*, 66-75.

Kumar, S. (2011). Transmission Loss Allocation and Loss Mininization by incorporating UPFC in LFA. *International Journal of Modern Engineering*, 236-245.

Kundur, P. (1994). Control of Active and reactive power. In P.Kundur, *Power System Stability and Control*,(2nd ed). British Columbia: McGraw-Hill.

Muthukrishnana, S. (2010). Comparison of simulation and experimental results of UPFC used fo power quality improvement. *International Journal of computer and Electrical Engineering*, 555-559.

National Laboratory of Engineering Science and Technology, (2011). *Reactive Power and Importance to Bulk Power System,2nd Edition.* Tennessee: Oak Ridge.

Nizam, M. (2006). Perfomance Evaluation of Voltage Stability Indices for Dynamic Voltage Collapse Prediction. *Journal of Applied Science*, 2558-2566.

Poornachandrarao, N.P. A. (2012). Improvement of power flow in the power system network by using UPFC device. *International Journal of Engineering research* , 1194-198.

Rani, C. A. (2012). Enhancement of power flow control and voltage stability in a power system by UPFC. *European Journal of scientific research*, 576-587.

Reddy, K. K. (2012). Transmission loss minimization using Advanced Unified power flow controller. *IOSR Journal of Engineering*, 1049-1052.

Reddy, K. M. (2012). Simulation of real,reactive power regulation with UPFC. *International journal of scientific research publications*, 23-33.

Renz, B. (1999). AEP Unified Power Flow Controller Perfomance. *IEEE*, 1374-1380.

Siganos, C. S. (2009). *Neural Networks,2nd edition.* Retrieved from Neural Networks, (2nd ed.) Retrieved from http://www.doc.ic.ac.uk/~nd/surprise_96/journal/vol4/cs11/report.html

Singh, S. (2012). The unified power flow controller optimal power flow model. *International Journal of Scientific and Research*, 1-3.

Tulasiram, G.S. A. (2008). Simulation of real and reactive power flow control with UPFC connected to a transmission line. *Journal of theoretical and applied information technology*, 16-22.

University, C. (2009). *Reactive Power Compesation of Transmission Lines,2nd Edition.* Winscosin: Concordia University.

University, L. (2001). *Reactive power valuation.* Scania: Lund University.

University, L. (2009). *Fundamentals of power Engineering:Lecture 10-Power flow studies,2nd Edition.* Texas: Lamar University.

USAID. (2010). *South Asia Regional Initiative for Energy.* New Delhi: USAID.

Vijayarpiya, P. (2010). Increasing the loadability and minimizing the losses using UPFC. *International Journal of Engineering Science and Technology*, 7343-7349.

Yokohama, Y. W. (2009). Assessment of optimal location of UPFC considering steady-state voltage stability. *The international conference on Electrical Engineering* (pp. 1-6). New Delhi: ICOEE.

APPENDICES

Appendix 1: IEEE 39-Bus, 10-Generator Test System

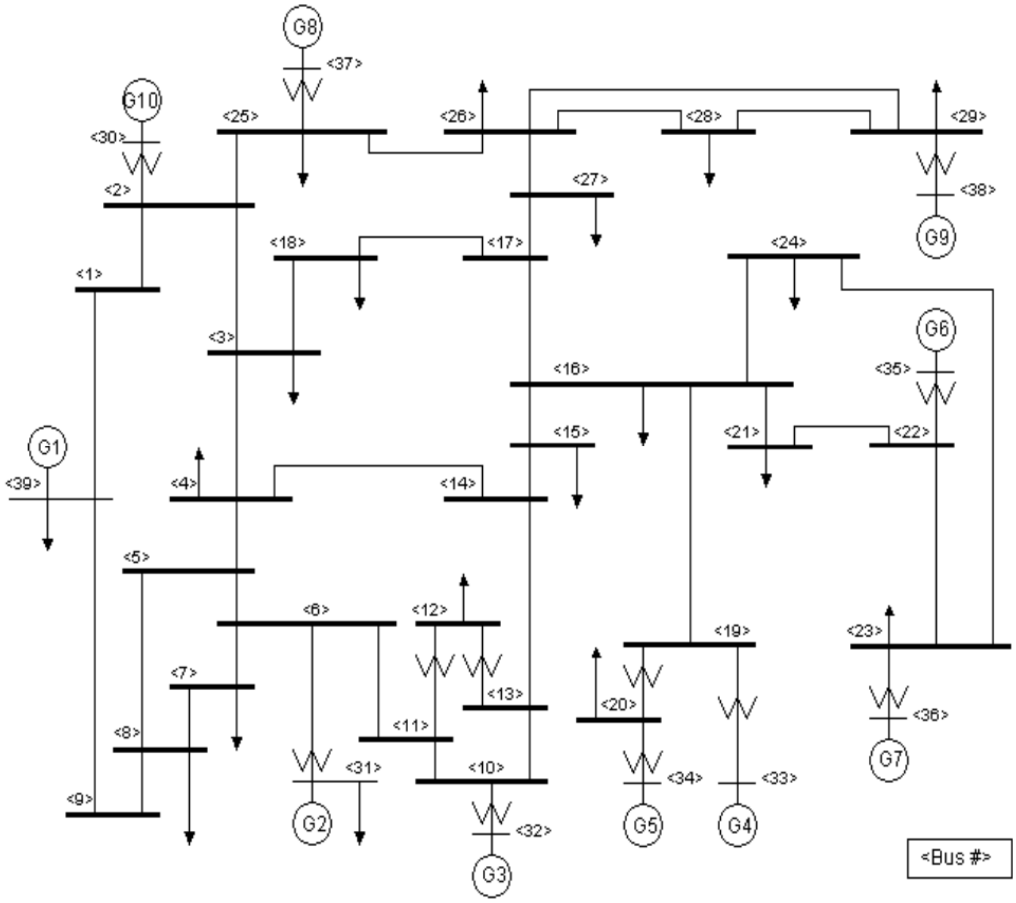

Fig.A1: The IEEE 10-Generators, 39-Bus system

Line Data					**Transformer Tap**	
From Bus	To Bus	R	X	B	Magnitude	Angle
1	2	0.0035	0.0411	0.6987	0	0
1	39	0.001	0.025	0.75	0	0
2	3	0.0013	0.0151	0.2572	0	0
2	25	0.007	0.0086	0.146	0	0
3	4	0.0013	0.0213	0.2214	0	0
3	18	0.0011	0.0133	0.2138	0	0
4	5	0.0008	0.0128	0.1342	0	0
4	14	0.0008	0.0129	0.1382	0	0
5	6	0.0002	0.0026	0.0434	0	0
5	8	0.0008	0.0112	0.1476	0	0
6	7	0.0006	0.0092	0.113	0	0
6	11	0.0007	0.0082	0.1389	0	0
7	8	0.0004	0.0046	0.078	0	0
8	9	0.0023	0.0363	0.3804	0	0
9	39	0.001	0.025	1.2	0	0
10	11	0.0004	0.0043	0.0729	0	0
10	13	0.0004	0.0043	0.0729	0	0
13	14	0.0009	0.0101	0.1723	0	0
14	15	0.0018	0.0217	0.366	0	0
15	16	0.0009	0.0094	0.171	0	0
16	17	0.0007	0.0089	0.1342	0	0
16	19	0.0016	0.0195	0.304	0	0
16	21	0.0008	0.0135	0.2548	0	0
16	24	0.0003	0.0059	0.068	0	0
17	18	0.0007	0.0082	0.1319	0	0
17	27	0.0013	0.0173	0.3216	0	0
21	22	0.0008	0.014	0.2565	0	0
22	23	0.0006	0.0096	0.1846	0	0
23	24	0.0022	0.035	0.361	0	0
25	26	0.0032	0.0323	0.513	0	0
26	27	0.0014	0.0147	0.2396	0	0
26	28	0.0043	0.0474	0.7802	0	0
26	29	0.0057	0.0625	1.029	0	0
28	29	0.0014	0.0151	0.249	0	0
12	11	0.0016	0.0435	0	1.006	0
12	13	0.0016	0.0435	0	1.006	0
6	31	0	0.025	0	1.07	0
10	32	0	0.02	0	1.07	0
19	33	0.0007	0.0142	0	1.07	0
20	34	0.0009	0.018	0	1.009	0
22	35	0	0.0143	0	1.025	0
23	36	0.0005	0.0272	0	1	0
25	37	0.0006	0.0232	0	1.025	0
2	30	0	0.0181	0	1.025	0
29	38	0.0008	0.0156	0	1.025	0
19	20	0.0007	0.0138	0	1.06	0

Table A.1: IEEE 39- Bus, 10-Generator,Lines and Transformer data

Bus	Type	Voltage	Load		Generator		
		[PU]	MW	MVar	MW	MVar	Unit No.
1	PQ	-	0	0	0	0	
2	PQ	-	0	0	0	0	
3	PQ	-	322	2.4	0	0	
4	PQ	-	500	184	0	0	
5	PQ	-	0	0	0	0	
6	PQ	-	0	0	0	0	
7	PQ	-	233.8	84	0	0	
8	PQ	-	522	176	0	0	
9	PQ	-	0	0	0	0	
10	PQ	-	0	0	0	0	
11	PQ	-	0	0	0	0	
12	PQ	-	7.5	88	0	0	
13	PQ	-	0	0	0	0	
14	PQ	-	0	0	0	0	
15	PQ	-	320	153	0	0	
16	PQ	-	329	32.3	0	0	
17	PQ	-	0	0	0	0	
18	PQ	-	158	30	0	0	
19	PQ	-	0	0	0	0	
20	PQ	-	628	103	0	0	
21	PQ	-	274	115	0	0	
22	PQ	-	0	0	0	0	
23	PQ	-	247.5	84.6	0	0	
24	PQ	-	308.6	-92	0	0	
25	PQ	-	224	47.2	0	0	
26	PQ	-	139	17	0	0	
27	PQ	-	281	75.5	0	0	
28	PQ	-	206	27.6	0	0	
29	PQ	-	283.5	26.9	0	0	
30	PV	1.0475	0	0	250	-	Gen10
31	PV	0.982	9.2	4.6	-	-	Gen2
32	PV	0.9831	0	0	650	-	Gen3
33	PV	0.9972	0	0	632	-	Gen4
34	PV	1.0123	0	0	508	-	Gen5
35	PV	1.0493	0	0	650	-	Gen6
36	PV	1.0635	0	0	560	-	Gen7
37	PV	1.0278	0	0	540	-	Gen8
38	PV	1.0265	0	0	830	-	Gen9
39	PV	1.03	1104	250	1000	-	Gen1

Table A.2: IEEE 39- Bus, 10-Generator Power and Voltage Set Points data

Appendix 2: Load Flow results (without UPFC)

BUS	V(p.u)	Phase(Degrees)	Pgen(p.u)	Qgen(p.u)	Pload(p.u)	Qload(p.u)
Bus1	1.0245	214.6961	0	0	0	0
Bus2	0.98947	217.8416	0	0	0	0
Bus3	0.95194	214.6903	0	0	3.22	0.024
Bus4	0.90526	213.6017	0	0	5	1.84
Bus5	0.90187	214.8966	0	0	0	0
Bus6	0.90193	215.7389	0	0	0	0
Bus7	0.8966	213.0345	0	0	2.3204	0.83366
Bus8	0.89894	212.4214	0	0	5.2077	1.7559
Bus9	0.98819	212.6792	0	0	0	0
Bus10	0.90592	218.8959	0	0	0	0
Bus11	0.90315	217.8187	0	0	0	0
Bus12	0.87809	217.8416	0	0	0.08091	0.83767
Bus13	0.90546	218.025	0	0	0	0
Bus14	0.9093	216.0139	0	0	0	0
Bus15	0.92199	215.7904	0	0	3.2	1.53
Bus16	0.94434	217.5952	0	0	3.29	0.323
Bus17	0.95075	216.2373	0	0	0	0
Bus18	0.94958	215.143	0	0	1.58	0.3
Bus19	0.93095	224.1213	0	0	0	0
Bus20	0.98095	223.0097	0	0	6.28	1.03
Bus21	0.95798	220.3569	0	0	2.74	1.15
Bus22	0.99261	225.3531	0	0	0	0
Bus23	0.99515	225.0953	0	0	2.475	0.846
Bus24	0.95532	217.7213	0	0	3.086	-0.92
Bus25	0.99871	219.4173	0	0	2.24	0.472
Bus26	0.98293	218.1797	0	0	1.39	0.17
Bus27	0.96147	215.9566	0	0	2.81	0.755
Bus28	0.98784	222.1331	0	0	2.06	0.276
Bus29	0.99109	225.2213	0	0	2.835	0.269
Bus30	1.0475	220.4085	2.5	1.8898	0	0
Bus31	0.982	224.6828	5.24	1.0297	0.092	0.046
Bus32	0.9831	227.8856	6.5	1.1018	0	0
Bus33	0.9972	230.0514	6.32	0.08195	0	0
Bus34	1.0123	228.2752	5.08	1.221	0	0
Bus35	1.0493	230.6014	6.5	2.5242	0	0
Bus36	1.0635	233.2886	5.6	2.9669	0	0
Bus37	1.0278	226.5907	5.4	0.37206	0	0
Bus38	1.0265	232.6813	8.3	0.77847	0	0
Bus39	1.03	212.96	10.0414	3.4753	11.04	2.5

Table A.3: Load flow results (Without UPFC)

From Bus	To Bus	Pflow(p.u)	Qflow(p.u)	Ploss(p.u)	Qloss(p.u)
2	1	1.276	-1.2564	0.00881	-0.60525
5	8	3.1358	0.01959	0.00968	0.01582
6	7	4.1664	0.3027	0.01289	0.10632
11	6	3.5954	-0.16353	0.0111	0.01692
7	8	1.8332	-0.63727	0.00185	-0.04154
8	9	-0.25032	-2.3478	0.01388	-0.12036
39	9	0.26703	1.0758	0.00283	-1.517
10	11	3.609	0.25135	0.00639	0.00901
10	13	2.891	-0.17932	0.00408	-0.01589
13	14	2.8125	-0.61538	0.00901	-0.04076
15	14	-0.10599	0.39271	0.00066	-0.29891
1	39	1.2672	-0.6511	0.00159	-0.75159
15	16	-3.094	-1.9227	0.01376	-0.00522
16	17	2.3207	-0.894	0.00477	-0.0598
16	19	-5.0137	1.2162	0.04838	0.32234
21	16	3.278	0.73488	0.01	-0.06179
24	16	0.43784	1.7259	0.00108	-0.04016
17	18	2.1018	-0.08411	0.00342	-0.079
17	27	0.21419	-0.7501	0.00059	-0.28612
22	21	6.0523	2.241	0.03429	0.35606
23	22	-0.44752	0.20064	0.00017	-0.17958
24	23	-3.5238	-0.80587	0.03092	0.14849
3	2	-3.5965	-2.079	0.02408	0.03727
26	25	-0.69648	-0.65189	0.00215	-0.48198
27	26	-2.5964	-1.219	0.01207	-0.09976
28	26	1.4146	-0.35794	0.00882	-0.66035
29	26	1.9176	-0.43323	0.02137	-0.76816
29	28	3.492	-0.13827	0.01738	-0.05633
2	25	-2.3966	0.85966	0.04727	-0.08621
3	4	0.89448	1.9386	0.00711	-0.0751
18	3	0.51835	-0.30511	0.00038	-0.18866
4	5	-1.4229	0.28989	0.00209	-0.07608
14	4	2.6968	0.117	0.00707	0.00018
6	5	4.5659	-0.31477	0.00515	0.03161
13	12	0.07439	0.45196	0.00041	0.01127
30	2	2.5	1.8898	0	0.17021
31	6	5.148	0.98372	0	0.81534
20	19	-1.2244	-0.29712	0.0013	0.02558
32	10	6.5	1.1018	0	1.0298
34	20	5.08	1.221	0.02441	0.48815
36	23	5.6	2.9669	0.01775	0.96585
35	22	6.5	2.5242	0	0.66346
33	19	6.32	0.08195	0.0322	0.65313
11	12	0.00726	0.40587	0.00035	0.00889
38	29	8.3	0.77847	0.05543	1.081
37	25	5.4	0.37206	0.01748	0.67602

Table A.4: Line flow results (Without UPFC)

Appendix 3: Load Flow results (with UPFC)

BUS	V(p.u)	Phase(Degrees)	Pgen(p.u)	Qgen(p.u)	Pload(p.u)	Qload(p.u)
Bus1	1.0245	214.7018	0	0	0	0
Bus2	0.98954	217.8645	0	0	0	0
Bus3	0.95203	214.7419	0	0	3.22	0.024
Bus4	0.90556	213.8309	0	0	5	1.84
Bus5	0.90186	214.931	0	0	0	0
Bus6	0.90183	215.7331	0	0	0	0
Bus7	0.89654	213.0459	0	0	2.3201	0.83355
Bus8	0.8989	212.4329	0	0	5.2072	1.7557
Bus9	0.98817	212.685	0	0	0	0
Bus10	0.90512	218.7125	0	0	0	0
Bus11	0.90261	217.6926	0	0	0	0
Bus12	0.87722	217.6525	0	0	0.08075	0.83602
Bus13	0.90422	217.7786	0	0	0	0
Bus14	0.90709	215.6071	0	0	0	0
Bus15	0.92092	215.5612	0	0	3.2	1.53
Bus16	0.94384	217.4405	0	0	3.29	0.323
Bus17	0.95048	216.1514	0	0	0	0
Bus18	0.94947	215.1086	0	0	1.58	0.3
Bus19	0.93079	223.9723	0	0	0	0
Bus20	0.98085	222.8607	0	0	6.28	1.03
Bus21	0.95764	220.2022	0	0	2.74	1.15
Bus22	0.99243	225.2042	0	0	0	0
Bus23	0.99496	224.9463	0	0	2.475	0.846
Bus24	0.9547	217.5723	0	0	3.086	-0.92
Bus25	0.99863	219.423	0	0	2.24	0.472
Bus26	0.98277	218.1396	0	0	1.39	0.17
Bus27	0.96124	215.8993	0	0	2.81	0.755
Bus28	0.98776	222.093	0	0	2.06	0.276
Bus29	0.99104	225.1812	0	0	2.835	0.269
Bus30	1.0475	220.4257	2.5	1.8862	0	0
Bus31	0.982	224.6828	5.24	1.0333	0.092	0.046
Bus32	0.9831	227.7023	6.5	1.1391	0	0
Bus33	0.9972	229.9024	6.32	0.09279	0	0
Bus34	1.0123	228.1263	5.08	1.2264	0	0
Bus35	1.0493	230.4525	6.5	2.5373	0	0
Bus36	1.0635	233.1397	5.6	2.9744	0	0
Bus37	1.0278	226.5964	5.4	0.37539	0	0
Bus38	1.0265	232.6412	8.3	0.7821	0	0
Bus39	1.03	212.96	10.0316	3.4761	11.04	2.5

Table A.5: Load flow results on Installation of UPFC

From Bus	To Bus	Pflow(p.u)	Qflow(p.u)	Ploss(p.u)	Qloss(p.u)
2	1	1.2822	-1.2554	0.00881	-0.60473
5	8	3.1582	0.02157	0.01006	0.01779
6	7	4.1469	0.29946	0.01252	0.10451
11	6	3.3753	-0.20165	0.00742	0.00181
7	8	1.814	-0.6386	0.00174	-0.04192
8	9	-0.24657	-2.3486	0.01375	-0.12025
39	9	0.26329	1.0767	0.00279	-1.1516
10	11	3.4073	0.21159	0.00443	0.00168
10	13	3.0927	-0.10424	0.00596	-0.00943
13	14	3.0328	-0.53927	0.01351	-0.02499
15	14	0.01612	0.43042	0.00082	-0.297
1	39	1.2733	-0.65067	0.0016	-0.75124
15	16	-3.2161	-1.9604	0.01642	0.00547
16	17	2.1975	-0.91061	0.00356	-0.06492
16	19	-5.0137	1.2001	0.04836	0.32219
21	16	3.2779	0.74509	0.01002	-0.06122
24	16	0.4378	1.7322	0.00108	-0.03993
17	18	2.0027	-0.09512	0.00253	-0.08262
17	27	0.19046	-0.75056	0.00054	-0.28613
22	21	6.0523	2.2523	0.03433	0.35717
23	22	-0.44755	0.19978	0.00017	-0.17951
24	23	-3.5238	-0.81218	0.03096	0.14949
3	2	-3.5675	-2.0816	0.0232	0.03388
26	25	-0.7204	-0.65146	0.00249	-0.48073
27	26	-2.6201	-1.2194	0.01262	-0.09763
28	26	1.4146	-0.35622	0.00882	-0.66013
29	26	1.9176	-0.43147	0.02137	-0.7679
29	28	3.492	-0.13649	0.01738	-0.05627
2	25	-2.3734	0.85618	0.0447	-0.08725
3	4	0.76675	1.935	0.00626	-0.07994
18	3	0.41955	-0.31251	0.00012	-0.18997
4	5	-1.2022	0.2936	0.00068	-0.08514
14	4	62.6397	67.6981	0	2.0254
6	5	4.3666	-0.3312	0.00389	0.02597
13	12	0.05523	0.44446	0.00039	0.0108
30	2	2.5	1.8862	0	0.16998
31	6	5.148	0.98727	0	0.81554
20	19	-1.2244	-0.29204	0.0013	0.02554
32	10	6.5	1.1391	0	1.0317
34	20	5.08	1.2264	0.02442	0.4883
36	23	5.6	2.9744	0.01777	0.96693
35	22	6.5	2.5373	0	0.66437
33	19	6.32	0.09279	0.0322	0.65316
11	12	0.02626	0.41155	0.00035	0.00919
38	29	8.3	0.7821	0.05543	1.0811
37	25	5.4	0.37539	0.01748	0.67608

Table A.6: Line flow results on Installation of UPFC